

Improved α^4 Term of the Electron Anomalous Magnetic Moment

Toichiro Kinoshita*

*Laboratory for Elementary Particle Physics
Cornell University, Ithaca, New York, 14853*

M. Nio†

Theoretical Physics Laboratory, RIKEN, Wako, Saitama, Japan 351-0198

(Dated: October 18, 2018)

Abstract

We report a new value of electron $g - 2$, or a_e , from 891 Feynman diagrams of order α^4 . The FORTRAN codes of 373 diagrams containing closed electron loops have been verified by at least two independent formulations. For the remaining 518 diagrams, which have no closed lepton loop, verification by a second formulation is not yet attempted because of the enormous amount of additional work required. However, these integrals have structures that allow extensive cross-checking as well as detailed comparison with lower-order diagrams through the renormalization procedure. No algebraic error has been uncovered for them. The numerical evaluation of the entire α^4 term by the integration routine VEGAS gives $-1.7283(35)(\alpha/\pi)^4$, where the uncertainty is obtained by careful examination of error estimates by VEGAS. This leads to $a_e = 1\,159\,652\,175.86\ (0.10)\ (0.26)\ (8.48) \times 10^{-12}$, where the uncertainties come from the α^4 term, the estimated uncertainty of α^5 term, and the inverse fine structure constant, $\alpha^{-1} = 137.036\,000\,3\ (10)$, measured by atom interferometry combined with a frequency comb technique, respectively. The inverse fine structure constant $\alpha^{-1}(a_e)$ derived from the theory and the Seattle measurement of a_e is $137.035\,998\,83\ (51)$.

PACS numbers: 13.40.Em, 14.60.Ef, 12.39.Fe, 12.40.Vv

*Electronic address: tk@hep.th.cornell.edu

†Electronic address: nio@riken.jp

I. INTRODUCTION AND SUMMARY

It was more than 18 years ago that an amazingly precise measurement of $g - 2$ values of the electron and positron in a Penning trap was reported [1]:

$$\begin{aligned} a_e^-(\text{exp}) &= 1\,159\,652\,188.4 (4.3) \times 10^{-12} \quad [3.7 \text{ ppb}], \\ a_e^+(\text{exp}) &= 1\,159\,652\,187.9 (4.3) \times 10^{-12} \quad [3.7 \text{ ppb}]. \end{aligned} \tag{1}$$

Numerals 4.3 in parentheses represent uncertainties in the last digits of measurements, and 3.7 ppb is the fractional precision (1 ppb = 1×10^{-9}). At present a new measurement of a_e , which is based on a cylindrical cavity whose property has been studied analytically [2], is in progress. It is expected to improve the precision substantially [3]. Unlike the muon $g - 2$, which is sensitive to short distance physics, the electron $g - 2$ is rather insensitive to short distance physics. It is therefore calculable to very high precision from the QED or, more generally, the Standard Model. High precision measurements of a_e thus enables us to subject the QED to a most stringent test. If disagreement is found between theory and experiment of a_e , it would have a very profound impact on the validity of QED, or modern quantum field theory in general. This is why high precision measurement of a_e is of such an importance.

The QED contribution to a_e can be written in general as

$$a_e(\text{QED}) = A_1 + A_2(m_e/m_\mu) + A_2(m_e/m_\tau) + A_3(m_e/m_\mu, m_e/m_\tau). \tag{2}$$

A_1, A_2, A_3 can be expanded as power series in α/π :

$$A_i = A_i^{(2)} \left(\frac{\alpha}{\pi}\right) + A_i^{(4)} \left(\frac{\alpha}{\pi}\right)^2 + A_i^{(6)} \left(\frac{\alpha}{\pi}\right)^3 + \dots, \quad i = 1, 2, 3. \tag{3}$$

$A_1^{(2)}, A_1^{(4)},$ and $A_1^{(6)}$ are known analytically [4, 5, 6] whose numerical values are

$$\begin{aligned} A_1^{(2)} &= 0.5, \\ A_1^{(4)} &= -0.328\,478\,965\,579 \dots, \\ A_1^{(6)} &= 1.181\,241\,456 \dots \end{aligned} \tag{4}$$

Actually, the analytic result $A_1^{(6)}$ is the culmination of a long sequence of analytic work that started around 1969 [7]. It took more than 25 years of hard work before it was finally completed by [6].

From the vantage of 1960 – 1970, analytic solution of the sixth-order muon $g-2$ diagrams containing an (external) light-by-light scattering subdiagram seemed to be extremely difficult. Thus, one of the authors (T.K.) and Aldins developed a numerical approach based on the technique of Feynman-parametric integral [8], calculating the integrand by hand. The subtle problem of renormalizing the light-by-light scattering subdiagram was bypassed taking advantage of gauge invariance. Meanwhile, Brodsky and Dufner were working on the same problem. We decided to join force and write the report together [9]. The resulting 7-dimensional integral was evaluated by an adaptive-iterative Monte-Carlo routine [10]. Sixth-order diagrams containing vacuum-polarization loops were also evaluated in a similar manner [11].

This method was then extended to general diagrams that require explicit renormalization [12, 13]. It consists of three steps:

(1) Conversion of momentum space integrals into integrals over Feynman parameters. This step is fully analytic and carried out by an algebraic manipulation software, such as SCHOONSCHIP [14] and FORM [15].

(2) Renormalization by a subtraction term that subtracts divergence *point-by-point* throughout the domain of integration. The renormalization term is constructed in such a way that it is analytically factorisable into products of a divergent part of renormalization constant and a $g-2$ term of lower order.

(3) Numerical integration by VEGAS [16], an improved version of adaptive-iterative Monte-Carlo integration routine [10].

We applied this scheme to two different formulations, both in Feynman gauge. One is to apply it to each vertex individually and add them up. Another starts by combining a set of vertices into one with the help of the Ward-Takahashi identity

$$q_\mu \Lambda^\mu(p, q) = -\Sigma(p + \frac{q}{2}) + \Sigma(p - \frac{q}{2}), \quad (5)$$

where $\Lambda^\mu(p, q)$ is the sum of vertices obtained by inserting the external magnetic field in fermion lines of a self-energy diagram $\Sigma(p)$. $p \pm q/2$ is outgoing (incoming) electron momentum. Differentiating both sides of (5) with respect to q_ν one obtains

$$\Lambda^\nu(p, q) \simeq -q^\mu \left[\frac{\partial \Lambda_\mu(p, q)}{\partial q_\nu} \right]_{q=0} - \frac{\partial \Sigma(p)}{\partial p_\nu}. \quad (6)$$

The magnetic projection of right-hand-side (RHS) provides the starting point of an independent formulation. This will be called *Version A* [17]. The approach starting from the left-hand-side will be called *Version B*. Although *Version A* requires additional algebraic work it results in fewer and more compact integrals than *Version B* and ensures significant economy of computing time.

The entire α^3 term was coded in both *Version A* and *Version B*. By 1974 this led to a crude estimate of $A_1^{(6)}$ [13]. To achieve a higher precision in this approach, however, very extensive computer work was required, which was not easily available at that time. It was only in 1995 that we were able to obtain a sufficiently precise result [18]

$$A_1^{(6)}(\text{num.}) = 1.181\,259\,(40). \quad (7)$$

Shortly afterwards this value was confirmed by the analytic result [6] to more than 5 digits.

Although analytic technique developed for integrating $A_1^{(6)}$, in particular that of integration by part, have been useful for analytic study of eighth-order term $A_1^{(8)}$, further development seems to be needed for a complete analytic integration of $A_1^{(8)}$ [19]. Only a small number of eighth-order diagrams without closed lepton loop have been integrated analytically thus far [20].

On the other hand, no theoretical difficulty has been encountered in the Feynman-parametric approach to $A_1^{(8)}$. The renormalization scheme developed in [12] for the sixth-order term could be readily extended to eighth-order. However, the enormous size of integrals of Group IV (see Sec. VI) and Group V (see Sec. VII) of eighth-order term and a large number of renormalization terms required presented a tremendous challenge to both algebraic construction of integrands and their evaluation by numerical means. For these reasons numerical evaluation of these diagrams were carried out initially in *Version A* only, which required smaller codes than *Version B*.

The first result of $A_1^{(8)}$ obtained by VEGAS [16]

$$A_1^{(8)} = -1.434(138) \quad (8)$$

was reported by 1990 [21, 22]. This was a very preliminary result based on about 10^7 sampling points per iteration and about 30 iterations. The estimated uncertainty of numerical evaluation was of the same order of magnitude as that of the experimental value [1].

In order to improve $A_1^{(8)}$ beyond (8) by an order of magnitude or more and move from a *qualitative* to *quantitative* calculation, it is necessary to evaluate the integrals using more

than two orders of magnitude of sampling points. It was estimated that this would require computation of up to ten years on high speed computers then available.

Because of this lengthy time scale and numerous requests for information on the status of calculation, preliminary values have been reported at several Conferences and Meetings and some of them have been printed in Proceedings and books:

$$\begin{aligned}
 A_1^{(8)} &= -1.557 \quad (70) && [23], \\
 A_1^{(8)} &= -1.4092 \quad (384), && [24], \\
 A_1^{(8)} &= -1.5098 \quad (384), && [25, 26], \\
 A_1^{(8)} &= -1.7366 \quad (60), && [27], \\
 A_1^{(8)} &= -1.7260 \quad (50), && [28, 29].
 \end{aligned}
 \tag{9}$$

Note that these values are not entirely independent. This is due to the fact that complete evaluation of each integral took typically three to six months of intense runs on fast computer. At any particular moment only a few of these integrals are being upgraded. The values in (9) are snapshots of this continuously evolving numerical work.

The difficulty encountered in improving numerical precision of $A_1^{(8)}$ turned out to be far greater than that of $A_1^{(6)}$. It was partly due to the enormous size of integrands, which made accumulation of good sampling of integrand difficult. However, the most serious problem we have encountered is that our method is very sensitive to the round-off error (called digit-deficiency or $d-d$ error) which is present in any computer calculation based on finite digit arithmetic, but affects our calculation particularly severely. (See Appendix B of Ref. [30] for details.) Because of these problems, some values given in (9) differ from each other considerably. For instance, the results of [25] and [24] differ by more than 2.6 s. d. Actually, error estimate of [25] generated by VEGAS was considerably smaller than that of [24]. However, unstable and erratic behavior of some integrals, in particular M_{40} discussed in detail in Sec. VII, indicated that the error estimate generated by VEGAS could not be trusted at face value. This is why the error assigned to [25] was enlarged to that of [24].

More recently, we discovered an algebraic error in the integrands formulated in *Version A* [26] while reevaluating 18 integrals of Group IV(d) by an independent formulation in *Version B*. Correction of this error is the cause of most of the jump from [25, 26] to [27].

The discovery of this error forced us to re-examine other diagrams, too. For this purpose, we have re-evaluated all diagrams of Groups IV(b) and IV(c) by an independent formulation in *Version B*. The result is that FORTRAN codes of all eighth-order $g-2$ diagrams containing

closed electron loops (373 diagrams) have now been verified by more than one independent formulations [17, 30]. Remaining 518 diagrams belonging to Group V, which have no closed lepton loops, have thus far been formulated only in *Version A*, because the amount of work required for *Version B* would be several times larger than that of *Version A*.

On the other hand, Group V diagrams are subject to very tight algebraic constraints. Namely, these diagrams have numerous renormalization terms which are constructed systematically by a power-counting rule that enables us to carry out an extensive cross-checking among themselves and with lower-order diagrams which are known exactly [22]. Having examined this procedure once again, we are convinced that they are completely free from algebraic error, although we found several typographical errors in the intermediate renormalization scheme described in Appendix C and Appendix D of [22]. These errors are corrected in Appendix B of this paper.

The really time-consuming task is to make sure that the result of numerical integration by VEGAS [16] can be trusted. This required a very good control of $d-d$ error. (See Appendix B of Ref. [30] for details.) This work has been carried out on a number of supercomputers over the period of more than 15 years. The latest results of this on-going effort are given in Eqs. (31), (37), (41), (52), and (58). Summing them up we obtain the total eighth-order term

$$A_1^{(8)} = -1.7283(35), \tag{10}$$

where the uncertainty is determined by careful analysis of errors estimated by VEGAS. This is an order of magnitude improvement over the previous value [25, 26].

At the level of precision we are interested in we cannot totally ignore the tenth-order term $A_1^{(10)}$, which is not known at present. In view of the gently increasing trend of coefficients of $(\alpha/\pi)^n$ as n increases from 1 to 4, however, it is unlikely that $A_1^{(10)}$ becomes suddenly very large. Following the argument of [31], let us assume, until proved otherwise, that

$$A_1^{(10)} = 0.0 \text{ (3.8)}. \tag{11}$$

In order to find out whether this is a justifiable assumption we have embarked on a very extensive project to evaluate $A_1^{(10)}$ [32, 33].

The electron anomaly receives also small mass-dependent contributions [34]

$$\begin{aligned}
A_2^{(4)}(m_e/m_\mu) &= 5.197\,386\,70\,(27) \times 10^{-7}, \\
A_2^{(4)}(m_e/m_\tau) &= 1.837\,63\,(60) \times 10^{-9}, \\
A_2^{(6)}(m_e/m_\mu) &= -7.373\,941\,58\,(28) \times 10^{-6}, \\
A_2^{(6)}(m_e/m_\tau) &= -6.5819\,(19) \times 10^{-8}, \\
A_3^{(6)}(m_e/m_\mu, m_e/m_\tau) &= 0.190\,95\,(63) \times 10^{-12},
\end{aligned} \tag{12}$$

where the uncertainties are due to measurement uncertainties of m_e/m_μ and m_e/m_τ only. Evaluation of $A_2^{(8)}(m_e/m_\mu)$, $A_2^{(8)}(m_e/m_\tau)$, and $A_3^{(8)}(m_e/m_\mu, m_e/m_\tau)$ are not difficult since we already have their codes. But, numerically, they are totally insignificant at present.

To evaluate the theoretical value of a_e we must also include non-QED contributions of the Standard Model [31, 35, 36]:

$$\begin{aligned}
a_e(\text{hadron}) &= 1.671\,(19) \times 10^{-12}, \\
a_e(\text{weak}) &= 0.030\,(1) \times 10^{-12}.
\end{aligned} \tag{13}$$

Although they are adequate for the moment, updates of these values would be desirable.

In order to compare theory with experiment we need a value of α , and the most precise one for that. Only recently such an α has become available by the progress of atom interferometry [37]. Combined with the measurement of the cesium $D1$ line [38], this leads to

$$\alpha^{-1}(h/M_{Cs}) = 137.036\,000\,3\,(10) \quad [7.4 \text{ ppb}]. \tag{14}$$

Using this α and a_e calculated from (10), (12), and (11) we obtain

$$a_e(h/M_{Cs}) = 1\,159\,652\,175.86\,(0.10)\,(0.26)\,(8.48) \times 10^{-12}, \tag{15}$$

where the first and second uncertainties are from (10) and (11), and the third is from (14).

This leads to

$$a_e(\text{exp}) - a_e(h/M_{Cs}) = 12.4\,(4.3)\,(8.5) \times 10^{-12}, \tag{16}$$

where first and second errors are from measurements of a_e and $\alpha(h/M_{Cs})$, respectively.

It is noted in [37] that the uncertainty 7.4 ppb in (14) may be brought down to 3.1 ppb when the nature of systematic error in the h/M_{Cs} measurement is understood better. This

is very exciting: The discrepancy (16) between theory and experiment would then become 2.2 s. d., which may provide the first serious challenge to the theory and measurement of a_e . Of course further work is needed to find out whether this is a real discrepancy or something else. The result of new measurement of a_e [3] is anxiously waited for.

An alternate and better test of QED is to compare α from (14) with α obtained from theory and measurement of a_e :

$$\begin{aligned}\alpha^{-1}(a_e) &= 137.035\,998\,834\ (12)\ (31)\ (502) \\ &= 137.035\,998\,834\ (503)\quad [3.7\ \text{ppb}],\end{aligned}\tag{17}$$

where, in the first line, 12 and 31 are uncertainties in theoretical values (10) and (11) and 502 is that of experimental value (1). This shows clearly that, if the measurement of a_e is improved by an order of magnitude, the precision of $\alpha(a_e)$ will be enhanced to about 0.3 ppb, putting it an order of magnitude ahead of $\alpha(h/M_{Cs})$ of (14). The current theoretical uncertainty in $(\alpha/\pi)^4 A_1^{(8)}$ is 0.10×10^{-12} , which is smaller than the uncertainty assumed for the $(\alpha/\pi)^5$ term. This means that more accurate evaluation of $A_1^{(8)}$ will not improve the QED prediction significantly until a better estimate of $A_1^{(10)}$ is obtained. Complete evaluation of $A_1^{(10)}$, which has contributions from 12672 Feynman diagrams, each of which may occupy FORTRAN code up to two orders of magnitudes larger than those of eighth-order terms, clearly requires an enormous amount of work [32, 33].

Appendix A describes how algebraic errors of Group V integrals are eliminated. Two-step renormalization scheme of Group V diagrams in Version A is described in Appendix B.

II. CLASSIFICATION OF DIAGRAMS CONTRIBUTING TO $A_1^{(8)}$

$A_1^{(8)}$ has contributions from 891 eighth-order vertex diagrams. Feynman integrals for these diagrams consist of twelve propagators integrated over 4 four-dimensional loop momenta. They may have subdiagrams of vacuum-polarization ($v-p$) type and/or light-by-light scattering ($l-l$) type. They fall into five gauge-invariant groups according to the type of proper vertex diagrams from which they are derived and the kind of closed electron loops they contain. The $v-p$ diagrams found in $A_1^{(8)}$ are as follows:

Π_2 , which consists of one closed lepton loop of second-order.

Π_4 , which consists of three proper closed lepton loops of fourth-order.

$\Pi_{4(2)}$, which consists of three lepton loops of type Π_4 whose internal photon line has a Π_2 insertion.

Π_6 , which consists of 15 proper closed lepton loops of sixth-order.

The l - l diagrams we need are:

Λ_4 , which consists of six proper closed lepton loops of fourth-order, with four photon lines attached to them.

$\Lambda_4^{(2)}$, which consists of 60 diagrams in which lepton lines and vertices of Λ_4 are modified by second-order radiative corrections.

We are now ready to classify the diagrams into five (gauge-invariant) groups:

Group I. Second-order electron vertex diagrams containing lepton v - p loops Π_2 , Π_4 , $\Pi_{4(2)}$ and/or Π_6 . This group consists of 25 diagrams.

Group II. Fourth-order proper vertex diagrams containing lepton v - p loops Π_2 and/or Π_4 . This group consists of 54 diagrams.

Group III. Sixth-order proper vertex diagrams containing a v - p loop Π_2 . This group consists of 150 diagrams.

Group IV. Vertex diagrams containing a light-by-light scattering subdiagram $\Lambda_4^{(2)}$ or Λ_4 with further radiative corrections of various kinds. This group has 144 diagrams, which can be divided further into subgroups IV(a), IV(b), IV(c), and IV(d).

Group V. Vertex diagrams with no closed electron loop. It consists of 518 diagrams.

Diagrams of Groups I, II, III and IV(a) are relatively easy to deal with since their structures are closely related to the second-, fourth-, and sixth-order diagrams, which are known exactly. They have been checked by several independent calculations [30].

In order to deal with the remaining diagrams in general, we need a full power of algebraic formulation originally developed for sixth-order diagrams [12] and extended to the eighth-order diagrams in [21]. But, for diagrams of Groups IV(b), IV(c), IV(d), as well as Group V, the *Version B* codes are so huge that we chose initially to work only with *Version A*. Since we fixed the error in Group IV(d) with the help of *Version B* calculation, however, we decided to evaluate Groups IV(b) and IV(c) in *Version B*, too. The numerical results are in excellent agreement with *Version A* [30].

This leaves Group V as the only group which has been evaluated in *Version A* only. Until it is evaluated in *Version B* or other methods, we have to rely on the very tight algebraic construction as the guarantor of the FORTRAN code of Group V.

III. GROUP I DIAGRAMS

Group I diagrams can be classified further into four gauge-invariant subgroups:

Subgroup I(a). Diagrams obtained by inserting three Π_2 's in a second-order vertex. This subgroup consists of one Feynman diagram. See Fig. 1(a).

Subgroup I(b). Diagrams obtained by inserting a Π_2 and a Π_4 in a second-order vertex. Six Feynman diagrams belong to this subgroup. See Fig. 1(b).

Subgroup I(c). Diagrams containing $\Pi_{4(2)}$. There are three Feynman diagrams that belong to this subgroup. See Fig. 2.

Subgroup I(d). Diagrams obtained by insertion of Π_6 in a second-order electron vertex. Fifteen Feynman diagrams belong to this subgroup. Eight are shown in Fig. 3. Diagrams *a, c, d, e, f* and the time-reversed diagram of *e* have charge-conjugated counterparts.

The evaluation of subgroups I(a) and I(b) is greatly facilitated by the analytic formulas available for the second- and fourth-order spectral representations of the renormalized photon propagators [39]. The contribution to a_e from the diagram obtained by sequential insertion of m k -th order electron and n l -th order electron v - p loops into a second-order electron vertex is reduced to a simple formula

$$a = \int_0^1 dy(1-y) \left[\int_0^1 ds \frac{\rho_k(s)}{1 + \frac{4}{1-s^2} \frac{1-y}{y^2} \left(\frac{m_e}{m_\mu}\right)^2} \right]^m \left[\int_0^1 dt \frac{\rho_l(t)}{1 + \frac{4}{1-t^2} \frac{1-y}{y^2}} \right]^n, \quad (18)$$

where ρ_k is the k -th order photon spectral function. Exact ρ_2 and ρ_4 can be found in Ref. [21, 39]. An exact spectral function for $\Pi_{4(2)}$ and an approximate one for Π_6 are also available [40, 41].

The contribution of diagrams of Fig. 1 can be obtained by choosing $(k = 2, m = 3, n = 0)$, $(k = 2, m = 2, l = 2, n = 1)$, $(k = 2, m = 1, l = 2, n = 2)$. The latest numerical values obtained by evaluating these integrals using VEGAS [16] are listed in Table I, where the number of sampling points per iteration and the number of iterations are also listed.

Note that these diagrams need no additional renormalization. Thus the renormalized amplitude $a_{2,p2:3}$ is given by

$$a_{2,p2:3} = M_{2,p2:3}. \quad (19)$$

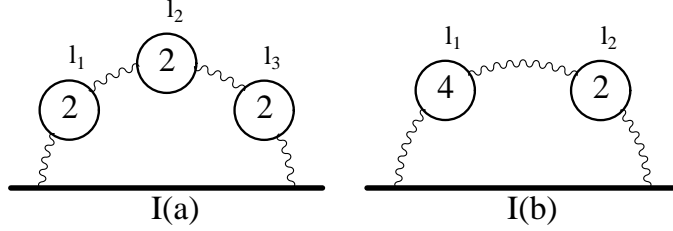


FIG. 1: (a) Diagrams contributing to subgroup I(a). (b) Diagrams contributing to subgroup I(b). Solid horizontal lines represent the electron in external magnetic field. Numerals “2”, “4” within solid circles refer to the proper renormalized v - p diagrams Π_2 and Π_4 , respectively. One and six Feynman diagrams contribute to I(a) and I(b), respectively.

From Table I, we obtain the contribution of subgroup I(a)

$$a_{I(a)}^{(8)} = 0.000\,876\,911\ (40), \quad (20)$$

which is 5 times more precise than the earlier result [42], and is in excellent agreement with the analytic result [43]:

$$a_{I(a)}^{(8)}(anal.) = 0.000\,876\,865\ \dots \quad (21)$$

The contributions of Fig. 1(b) for $(l_1, l_2) = (e, e)$ can be written down in a similar fashion. The most recent result of numerical integration by VEGAS is listed in the second row of Table I:

$$a_{I(b)}^{(8)} = 0.015\,325\,6\ (6). \quad (22)$$

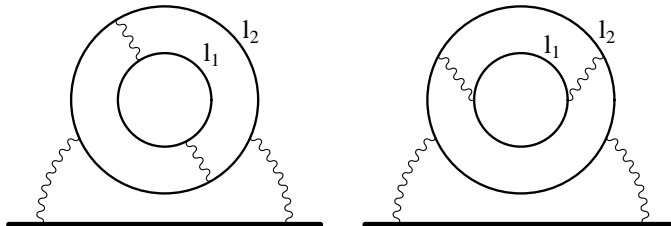


FIG. 2: Diagrams contributing to subgroup I(c). $(l_1, l_2) = (e, e)$. See FIG. 1 for notation.

In evaluating the contribution to a_e from the 9 Feynman diagrams of subgroup I(c) shown in FIG. 2, our approach is to make use of the parametric integral representation of the v - p

TABLE I: Contributions of diagrams of Figs. 1(a), 1(b), and 3. n_F is the number of Feynman diagrams represented by the integral. Evaluation was carried out on α workstations in 1997.

Integral	n_F	Value (Error) including n_F	Sampling per iteration	No. of iterations
$M_{2,P2:3}$	1	0.876 911 (40) $\times 10^{-3}$	1×10^7	55
$M_{2,P2,P4}$	6	0.015 325 6 (6)	1×10^7	55
$\Delta M_{2,P4a(P2)}$	1	0.011 403 1 (8)	1×10^7	64
$\Delta M_{2,P4b(P2)}$	2	0.001 716 8 (4)	1×10^7	55
$\Delta M_{2,P6a}$	2	0.044 448 (3)	1×10^8	70
$\Delta M_{2,P6b}$	1	0.028 594 (3)	1×10^8	70
$\Delta M_{2,P6c}$	2	-0.038 374 (2)	1×10^8	70
$\Delta M_{2,P6d}$	2	-0.027 507 (2)	1×10^8	70
$\Delta M_{2,P6e}$	4	0.179 335 (3)	4×10^8	70
$\Delta M_{2,P6f}$	2	-0.062 004 (2)	1×10^8	70
$\Delta M_{2,P6g}$	1	0.038 879 (2)	1×10^8	70
$\Delta M_{2,P6h}$	1	0.023 675 (2)	1×10^8	70

term $\Pi_{4(2)}$. Following the two-step renormalization procedure, these contributions can be written in the form [44]

$$a_{2,P4(P2)} = \Delta M_{2,P4a(P2)} + \Delta M_{2,P4b(P2)} - 2\Delta B_{2,P2}M_{2,P2}, \quad (23)$$

where each term is finite integral obtained by the \mathbf{K}_S renormalization procedure described in Ref. [21, 30]. The suffix $P2$ stands for the second-order v - p diagram Π_2 , $P4$ for the fourth-order v - p diagram Π_4 , while $P4(P2)$ represents the diagram $\Pi_{4(2)}$. $P4$ receives contributions from P_{4a} (vertex correction) and P_{4b} (two lepton self-energy insertions), $P4 = P_{4a} + P_{4b}$.

The results of numerical evaluation of (23), obtained by VEGAS, are listed in Table I. Note that the value listed in column 3 for $\Delta M_{2,P4b(P2)}$ includes the factor n_F . Numerical

TABLE II: Auxiliary integrals for Group I. Some integrals are known exactly. Remaining integrals are obtained numerically by VEGAS.

Integral	Value (Error)	Integral	Value (Error)
$M_{2,P2}$	0.015 687 421 ...	$M_{2,P2^*}$	-0.012 702 383 ...
$\Delta M_{2,P4}$	0.076 401 785 ...		
ΔB_2	0.75	$\Delta B_{2,P2}$	0.063 399 266 ...
ΔL_4	0.465 024 (17)	ΔB_4	-0.437 094 (21)
$\Delta \delta m_4$	1.906 340 (21)		

values of lower-order Feynman integrals, in terms of which the residual renormalization terms are expressed, are given in Table II. From these Tables we obtain

$$a_{Ic}^{(8)} = 0.011\,130\,8\,(9). \quad (24)$$

We obtained an independent check of (24) using a two-dimensional integral form of α^3 spectral function for $\Pi_{4(2)}$ of Fig. 2, which was derived from the QCD spectral function obtained in [40]. Numerical integration using this spectral function gives

$$a_{Ic}^{(8)} = 0.011\,131\,2\,(12), \quad (25)$$

for 10 million sampling points iterated 20 times in quadruple precision. This is in agreement with (24) to the fifth decimal points although their approaches are quite different.

The new result (24) confirms the old result [22] but with a much higher precision.

The contribution to a_e from 15 diagrams of subgroup I(d) (see Fig. 3) can be written as

$$a_{2,P6i} = \Delta M_{2,P6i} + \text{residual renormalization terms}, \quad (i = a, \dots, h). \quad (26)$$

Divergence-free integrals $\Delta M_{2,P6i}$ are defined by (4.13) of Ref. [21]. Their numerical values (summed over the diagrams related by time-reversal and charge-conjugation symmetries) are evaluated numerically by VEGAS and listed in the third column of Table I.

Summing up the contributions of diagrams $P6a$ to $P6h$ of Fig. 3, we obtain the following expression:

$$\begin{aligned} a_{I(d)}^{(8)} &= \sum_{i=a}^h \Delta M_{2,P6i} - 4\Delta B_2 \Delta M_{2,P4} \\ &+ 5(\Delta B_2)^2 M_{2,P2} - 2(\Delta L_4 + \Delta B_4) M_{2,P2} \\ &- 2\Delta \delta m_4 M_{2,P2^*}, \end{aligned} \quad (27)$$

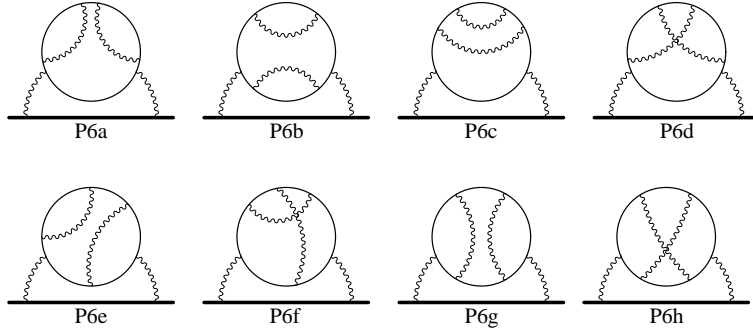


FIG. 3: Eighth-order vertices of subgroup I(d) obtained by insertion of sixth-order (single electron loop) v - p diagram Π_6 in a second-order electron vertex.

where the value of $\Delta M_{2,P6i}$ in column 3 of Table I is the sum of n_F vertex diagrams and

$$\begin{aligned}
\Delta B_2 &= \Delta' B_2 + \Delta' L_2 = \frac{3}{4}, \\
\Delta M_{2,P4} &= \Delta M_{2,P4a} + 2\Delta M_{2,P4b}, \\
\Delta L_4 &= \Delta L_{4x} + 2\Delta L_{4c} + \Delta L_{4l} + 2\Delta L_{4s}, \\
\Delta B_4 &= \Delta B_{4a} + \Delta B_{4b}, \\
\Delta \delta m_4 &= \Delta \delta m_{4a} + \Delta \delta m_{4b}.
\end{aligned} \tag{28}$$

The quantities listed in (28) are defined in Ref. [21]. Their numerical values are listed in Table II. The 1998 results of numerical integration of $\Delta M_{2,P6i}$ are listed in Table I. From the numerical values in Tables I and II we obtain

$$a_{I(d)}^{(8)} = 0.049\,516\,1\,(63). \tag{29}$$

We obtained an independent check of (29) using the *Padé* approximant of the sixth-order photon spectral function [41]

$$a_{I(d)}^{(8)}(\textit{Padé}) = 0.049\,519\,5\,(38), \tag{30}$$

which is in excellent agreement with (29). Calculation was carried out in real*16 for 10 million sampling points iterated 100 times.

Collecting the results (21), (22), (24) and (29), we find the best value of the contribution to the electron anomaly from the 25 diagrams of group I to be

$$A_1^{(8)}[I] = 0.076\,849\,(7). \tag{31}$$

IV. GROUP II DIAGRAMS

Diagrams of this group are generated by inserting Π_2 and Π_4 in the photon lines of fourth-order vertex diagrams. Use of analytic expressions for the second- and fourth-order spectral functions for the photon propagators and time-reversal symmetry cuts down the number of independent integrals in *Version A* from 54 to 8.

The contribution to a_e arising from the set of vertex diagrams represented by the “self-energy” diagrams of Fig. 4 can be written in the form

$$a_{4,P_\alpha} = \Delta M_{4,P_\alpha} + \text{residual renormalization terms}, \quad (32)$$

where $\Delta M_{4,P_\alpha}$ are finite integrals obtained in the intermediate step of two-step renormalization [22]. Their numerical values, obtained by VEGAS are listed in Table III. The values of auxiliary integrals needed to calculate the total contribution of group II diagrams are given in Tables II and IV.

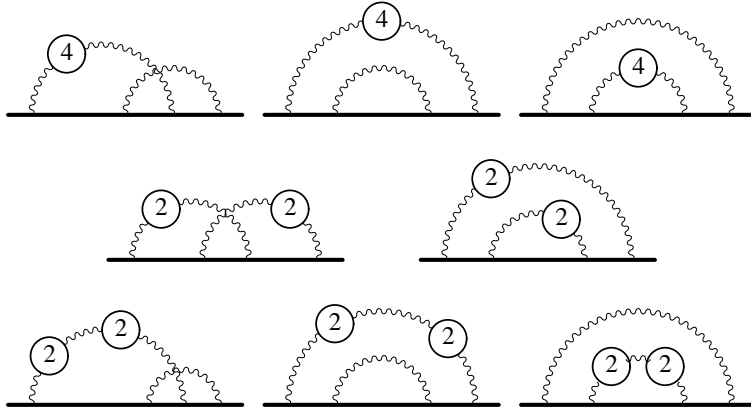


FIG. 4: Eighth-order diagrams obtained from the fourth-order vertex diagrams by inserting vacuum-polarization loops Π_2 and Π_4 .

Summing the contributions of diagrams of the first, second, and third rows of Fig. 4, one obtains (see Ref. [22] for notation)

$$\begin{aligned} a_{4,P_4} &= \Delta M_{4a,P_4} + \Delta M_{4b,P_{1':4}} + \Delta M_{4b,P_{0:4}} \\ &- \Delta B_2 M_{2,P_4} - \Delta B_{2,P_4} M_2, \end{aligned} \quad (33)$$

TABLE III: Contributions of diagrams of Fig. 4. n_F is the number of Feynman diagrams represented by the integral. Suffixes $P0$ and $P1'$ are remnants of notations in [22] and refer to two virtual photons in which v-p insertions are made. Numerical evaluation was carried out on α workstations in 2001.

Integral	n_F	Value (Error) including n_F	Sampling per iteration	No. of iterations
$\Delta M_{4a,P4}$	18	0.131 298 (8)	2×10^9	100
$\Delta M_{4b,P0:4}$ + $\Delta M_{4b,P1':4}$	18	-0.420 295 (8)	4×10^8	100
$\Delta M_{4a,P2,P2}$	3	-0.004 351 (2)	1×10^8	70
$\Delta M_{4b,P1':2,P0:2}$	3	-0.022 332 (1)	1×10^8	70
$\Delta M_{4a,P2:2}$	6	0.007 875 (8)	2×10^8	70
$\Delta M_{4b,P0:2:2}$ + $\Delta M_{4b,P1':2:2}$	6	-0.065 458 (4)	1×10^8	70

$$a_{4,P2,P2} = \Delta M_{4a,P2,P2} + \Delta M_{4b,P1':2,P0:2} - \Delta B_{2,P2} M_{2,P2}, \quad (34)$$

$$a_{4,P2:2} = \Delta M_{4a,P2:2} + \Delta M_{4b,P1':2:2} + \Delta M_{4b,P0:2:2} - \Delta B_2 M_{2,P2:2} - \Delta B_{2,P2:2} M_2, \quad (35)$$

respectively, where $M_{2,P4}$ is equal to $\Delta M_{2,P4} - 2\Delta B_2 M_{2,P2}$. $M_{4a,\dots}$ corresponds to the left-most diagrams of Fig. 4 and $M_{4b,\dots}$ ones on the right. $\Delta M_{4a,\dots}$ is the sum of n_F vertex diagrams. On the other hand, the auxiliary integrals listed in Tables II and IV do not include multiplicity.

Substituting the data from Tables II and III into (33), (34), and (35) we obtain

$$\begin{aligned} a_{4,P4} &= -0.420 483 (12), \\ a_{4,P2,P2} &= -0.027 677 (2), \\ a_{4,P2:2} &= -0.073 452 (9). \end{aligned} \quad (36)$$

Note that values listed in column 3 of Table III include the factor n_F .

TABLE IV: Auxiliary integrals for Group II. Some integrals are known exactly. Remaining integrals are obtained by VEGAS integration, with total sampling points of order 10^{11} .

Integral	Value (Error)	Integral	Value (Error)
M_2	0.5	$M_{2,P4}$	0.052 870 652 \dots
$M_{2,P2:2}$	0.002 558 524 \dots		
$\Delta B_{2,P4}$	0.183 666 5 (18)	$\Delta B_{2,P2:2}$	0.027 902 3 (4)

The sum of contributions of 54 diagrams of group II is

$$a_{II}^{(8)} = -0.521\,613\,(15). \quad (37)$$

V. GROUP III DIAGRAMS

Diagrams belonging to this group are generated by inserting a second-order vacuum-polarization loop Π_2 in the photon lines of sixth-order electron vertex diagrams of the three-photon-exchange type. Time-reversal invariance and use of the function ρ_2 (see (18)) for the photon spectral function reduce the number of independent integrals in *Version A* from 150 to 8. Some of these integrals are represented by the “self-energy” diagrams of Fig. 5.

Let $M_{6\alpha,P2}$ be the magnetic moment projection in *Version A* of the set of 150 diagrams generated from a self-energy diagram α (=A through H) of Fig. 5 by insertion of Π_2 and an external vertex. The renormalized contribution due to the group III diagrams can then be written as

$$a_{III}^{(8)} = \sum_{\alpha=A}^H a_{6\alpha,P2}, \quad (38)$$

where

$$a_{6\alpha,P2} = \Delta M_{6\alpha,P2} + \text{residual renormalization terms.} \quad (39)$$

$\Delta M_{6\alpha,P2}$ is UV- and IR-finite: all divergences of $M_{6\alpha,P2}$ have been projected out by \mathbf{K}_S and \mathbf{I}_R operations. (See Ref. [22].)

The latest numerical values of Group III integrals are summarized in Table V. Numerical values of auxiliary integrals needed in the renormalization scheme are listed in Tables II, IV

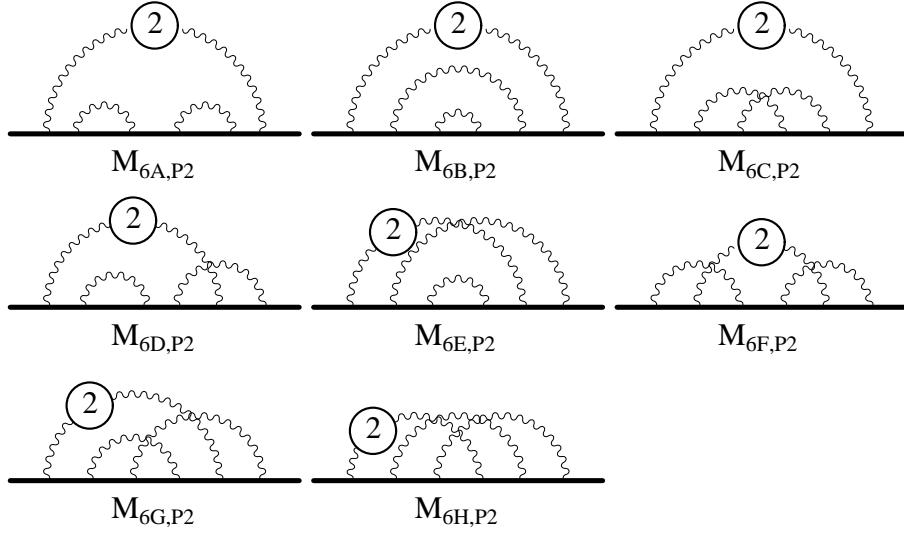


FIG. 5: Typical eighth-order diagrams obtained by insertion of a vacuum-polarization loop Π_2 in electron diagrams of the three-photon-exchange type. Altogether there are 150 diagrams of this type.

and VI. For comparison, the results of old calculation [42] carried out in double precision are listed in the last column of Table V. This is to examine the effect of *digit-deficiency* error. In this case the effect is relatively mild because the introduction of a vacuum-polarization loop tends to make the integrand less sensitive to the singularity.

When summed over all the diagrams of group III, the UV- and IR-divergent pieces cancel out and the total contribution to a_e can be written as a sum of finite pieces (see Ref. [22] for notation):

$$\begin{aligned}
a_{III}^{(8)} &= \sum_{\alpha=A}^H \Delta M_{6\alpha,P2} \\
&- 3\Delta B_{2,P2}\Delta M_4 - 3\Delta B_2\Delta M_{4,P2} \\
&+ (M_{2^*,P2}[I] - M_{2^*,P2})\Delta\delta m_4 + (M_{2^*}[I] - M_{2^*})\Delta\delta m_{4,P2} \\
&- M_{2,P2}[\Delta B_4 + 2\Delta L_4 - 2(\Delta B_2)^2] \\
&- M_2(\Delta B_{4,P2} + 2\Delta L_{4,P2} - 4\Delta B_2\Delta B_{2,P2}), \tag{40}
\end{aligned}$$

where $\Delta M_{6\alpha,P2}$ listed in Table V is the sum of n_F vertex diagrams. M_{2^*} is the magnetic moment obtained from M_2 by insertion of a two-point vertex in the electron lines. $M_{2^*}[I]$ is

TABLE V: Contributions of diagrams of Fig. 5. n_F is the number of Feynman diagrams represented by the integral. Integrals were evaluated in double precision except for a small part of $\Delta M_{6G,P2}$ which was evaluated in quadruple precision.

Integral	n_F	Value (Error) including n_F	Sampling per iteration	No. of iterations	Data from Ref. [42]
$\Delta M_{6A,P2}$	5	-0.440 307 (56)	1×10^8	97	-0.440 3 (3)
$\Delta M_{6B,P2}$	5	0.689 660 (84)	2×10^8	100	0.690 7 (7)
$\Delta M_{6C,P2}$	5	0.638 503 (80)	2×10^8	100	0.638 2 (7)
$\Delta M_{6D,P2}$	10	0.440 999 (77)	2×10^8	100	0.442 0 (7)
$\Delta M_{6E,P2}$	5	0.431 541 (55)	1×10^8	100	0.432 1 (4)
$\Delta M_{6F,P2}$	5	0.442 163 (83)	2×10^8	100	0.441 9 (8)
$\Delta M_{6G,P2}$	10	1.140 811 (76)			1.140 4 (10)
<i>d-part</i>		1.054 635 (60)	2×10^8	100	
<i>q-part</i>		0.086 176 (47)	2×10^7	100	
$\Delta M_{6H,P2}$	5	-0.797 941 (83)	6×10^8	100	-0.797 5 (12)

TABLE VI: Auxiliary integrals for Group III. Some integrals are known exactly. Remaining integrals are obtained by VEGAS integration, with total sampling points of order 10^{11} .

Integral	Value (Error)	Integral	Value (Error)
M_{2^*}	1.0	$M_{2^*}[I]$	-1.0
$M_{2^*,P2}$	0.044 077 4 (3)	$M_{2^*,P2}[I]$	0.010 255 3 (11)
ΔM_4	0.030 833 612 ...	$\Delta M_{4,P2}$	-0.106 707 082 ...
$\Delta \delta m_4$	1.906 340 (21)	$\Delta \delta m_{4,P2}$	0.679 769 (15)
$\Delta B_{4,P2} + 2\Delta L_{4,P2}$	0.085 865 (30)		

the part of M_{2^*} which may be IR-divergent according to the IR power counting. An analytic evaluation of $M_{2^*}[I]$ turns out to be finite and is listed in Table VI.

Plugging the values listed in Tables II, IV and VI in (40), we obtain

$$a_{III}^{(8)} = 1.417 722 (214). \quad (41)$$

VI. GROUP IV DIAGRAMS

Diagrams of this group can be divided into four subgroups: IV(a), IV(b), IV(c), and IV(d). Each subgroup consists of two equivalent sets of diagrams related by charge conjugation (reversal of the direction of momentum flow in the loop of the light-by-light scattering subdiagram). Diagrams of subgroups IV(a), IV(b), and IV(c) are obtained by modifying the sixth-order diagram M_{6LL} which contains the light-by-light scattering subdiagram Λ_4 , one of whose external photon line represents the magnetic field. The magnetic moment contribution M_{6LL} is known analytically [45], whose numerical value is

$$M_{6LL} = 0.371\ 005\ 292\dots \quad (42)$$

Subgroup IV(a). Diagrams obtained by inserting a second-order vacuum-polarization loop Π_2 in M_{6LL} . This subgroup consists of 18 vertex diagrams. In *Version A* they are represented by the self-energy-like diagrams shown in Fig. 6. Insertion of the magnetic vertex in these figures generates diagrams of *Version B*. Since M_{6LL} is known analytically and since insertion of Π_2 is straightforward, this subgroup is known exactly.

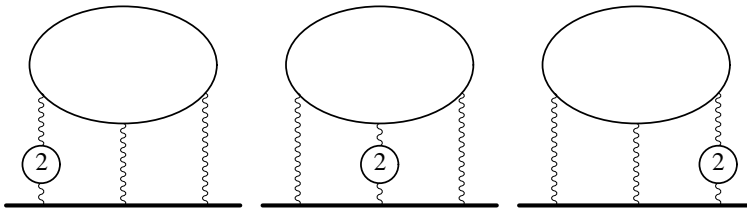


FIG. 6: Electron self-energy-like diagrams representing the external-vertex-summed integrals of subgroup IV(a). $(l_1, l_2) = (e, e)$.

Subgroup IV(b). Diagrams containing sixth-order light-by-light scattering subdiagrams $\Lambda_{4(2)}$. Altogether, there are 60 diagrams of this type. Charge-conjugation and time-reversal symmetries and summation over external vertex insertions reduce the number of independent integrals to 4 in *Version A*, represented by the self-energy-like diagrams LLA, LLB, LLC and LLD of Fig. 7. They can be generated from a common template by permutation of tensor indices of virtual photons attached to the $\Lambda_4^{(2)}$ loop. Similarly, all diagrams of *Version B* can be generated from a common template.

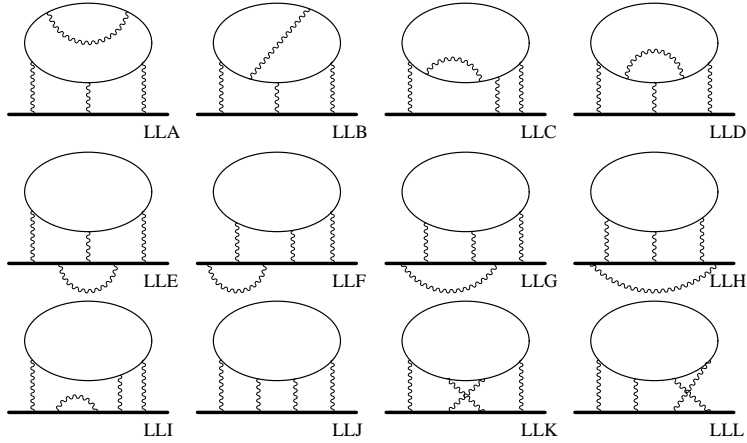


FIG. 7: Electron self-energy-like diagrams representing (external-vertex-summed) integrals of subgroup IV(b), IV(c), and IV(d).

Subgroup IV(c). Diagrams obtained by including second-order radiative corrections on the open electron line of M_{6LL} . There are 48 diagrams that belong to this subgroup. Summation over external vertex insertions and use of the interrelations available due to charge-conjugation and time-reversal symmetries leave five independent integrals in *Version A*, represented by the self-energy-like diagrams LLE, LLF, LLG, LLH and LLI of Fig. 7. They can be generated from a common template by permutation of tensor indices of virtual photons attached to the open electron line. Similarly, all diagrams of *Version B* can be generated from a common template.

Subgroup IV(d). Diagrams generated by inserting Λ_4 *internally* in fourth-order vertex diagrams. Diagrams of this type appear for the first time in the eighth order. Charge-conjugation invariance and summation over the external vertex insertion with the help of the Ward-Takahashi identity lead us to three independent integrals in *Version A*, represented by the diagrams LLJ, LLK and LLL of Fig. 7. They can be generated from a common template by permutation of tensor indices of virtual photons attached to the Λ_4 loop. Similarly, all diagrams of *Version B* can be generated from a common template.

In subgroups IV(a), IV(b), and IV(c) UV-divergences arising from the light-by-light scattering subdiagram Λ_4 , or more explicitly $\Pi^{\nu\alpha\beta\gamma}(q, k_i, k_j, k_l)$, can be taken care of by making

use of the identity:

$$\Pi^{\nu\alpha\beta\gamma}(q, k_i, k_j, k_l) = - q_\mu \left[\frac{\partial}{\partial q_\nu} \Pi^{\mu\alpha\beta\gamma}(q, k_i, k_j, k_l) \right], \quad (43)$$

which follows from the Ward-Takahashi identity. Namely, no explicit UV renormalization is needed if one uses the RHS of (43) instead of LHS and the fact that $\Sigma(p)$ of (6) vanishes by Furry's theorem. On the other hand, $\Sigma(p)$ is nonzero for subgroup IV(d) and the UV-divergence associated with the light-by-light scattering subdiagram Λ_4 must be regularized, e. g., by dimensional regularization. For these diagrams it is necessary to carry out explicit renormalization of Λ_4 as well as that of the two sixth-order vertex subdiagrams containing Λ_4 . See [17] for a detailed discussion of renormalization based on a combination of dimensional regularization and Pauli-Villars regularization.

Many diagrams of Groups IV(b) and IV(c) have UV divergences associated with the second-order vertex or self-energy parts. Their renormalization is achieved by a subtraction term which can be factorized analytically into a product of UV-divergent part of the renormalization constant and the sixth-order amplitude M_{6LL} (in *Version A*) or its component (in *Version B*). This enables us to verify the analytic structure of many terms of the integrand. A similar argument applies to diagrams with IR divergence. Since different diagrams generated by the same template have different divergences, this procedure explores the validity of template itself exhaustively.

On the other hand, Group IV(d) diagrams LLJ, LLK, and LLL have no UV-divergent subdiagram of second-order. Thus they could not be verified by comparison with known lower-order structure. Indeed, this is why the errors in 18 integrals of Group IV(d) remained undetected until the integrand was constructed in *Version B* [17]. The error was in the template of Group IV(d) where some non-divergent terms were left out inadvertently.

The argument presented above suggests that the validity of codes for Groups IV(b) and IV(c) can be established within *Version A*. However, as a further check, we have also evaluated them in *Version B*. In the following let us consider *Version A* and *Version B* separately since renormalization is handled slightly differently in two cases.

A. Version A

The calculation of group IV(a) contribution is particularly simple. This is because M_{6LL} has been fully tested by comparison with the analytic result [45], and insertion of the vacuum polarization term is straightforward. As a consequence the integral $M_{6LL,P2}$ is finite, which means

$$a_{6LL,P2} = M_{6LL,P2} = \Delta M_{6LL,P2}. \quad (44)$$

The result of numerical calculation is listed in Table VI.

Let us denote magnetic projections of subgroups IV(b) and IV(c) as $M_{8LL\alpha}$ where $\alpha = A, \dots, I$. Relating the IR- and UV-divergent $M_{8LL\alpha}$ to the finite, numerically calculable piece $\Delta M_{8LL\alpha}$ defined by the procedure of two-step renormalization of Ref. [46], one can write the contributions of the diagrams of subgroups IV(b) and IV(c) as

$$a_{IV(b)}^{(8)} = \sum_{\alpha=A}^D \Delta M_{8LL\alpha} - 3\Delta B_2 M_{6LL}, \quad (45)$$

and

$$a_{IV(c)}^{(8)} = \sum_{\alpha=E}^I \Delta M_{8LL\alpha} - 2\Delta B_2 M_{6LL}, \quad (46)$$

where the six-order light-by-light contribution to the anomaly is given by (42), and $\Delta M_{8LL\alpha}$ listed in Table VII represents the sum of n_F diagrams.

Numerical integration of all terms contributing to $a_{IV}^{(8)}$ has been carried out using VEGAS [16]. The latest results for Groups IV(b) and IV(c) are listed in Table VII. The result for Group IV(d) had been handled separately [17]. In general, the major difficulty in dealing with the diagrams of Groups IV(b) and IV(c) arises from the enormous size of integrands (up to 5000 terms and 240 kilobytes of FORTRAN source code per integral) and the large number of integration variables (up to 10).

Unlike $A_2^{(8)}(m_\mu/m_e)$ for muon $g-2$, which has a singular surface just outside of the integration domain (unit cube), the singularity of the mass-independent $A_1^{(8)}$ is far away from the domain of integration. This makes evaluation of electron $g-2$ less sensitive to the *digit-deficiency* problem. Nevertheless, our point-wise renormalization scheme is susceptible to the *d-d* problem.

TABLE VII: Contributions of diagrams of Fig. 6 and Fig. 7 excluding LLJ, LLK, and LLL which were evaluated separately in Ref. [17]. n_F is the number of Feynman diagrams represented by the integral. Some integrals are split into two parts: *d-part* is evaluated in real*8 and *q-part* is evaluated in real*16. *a-part* refers to the adjustable precision method developed by [48]. The superscript * indicates that indicated contributions were obtained by extrapolation from calculations in which the edges of integration domain were chopped off by 1.d-10. See Appendix B of Ref. [30] for details. Numerical work was carried out on SP3, velocity cluster, SP2, Condor cluster, and α workstations over several years. The table lists only the latest of results obtained by various means.

Integral	n_F	Value (Error) including n_F	Sampling per iteration	No. of iterations
$\Delta M_{6LL,P2}$	6	0.598 948 (137)	4×10^8	100
ΔM_{8LLA}	10	0.171 527 (292)		
<i>d-part</i>		0.148 729 (268)	2×10^8	100
<i>q-part</i>		0.022 798 (116)	2×10^5	380
ΔM_{8LLB}	20	- 1.296 116 (481)	2×10^8	99
ΔM_{8LLC}	20	2.840 029 (513)		
<i>d-part</i>		2.705 399 (345)	1×10^9	60
<i>q-part1</i>		0.132 081 (375)	4×10^6	63
<i>q-part2</i>		0.002 549 (53)	1×10^6	100
ΔM_{8LLD}	10	- 0.058 890 (325)	2×10^8	100
ΔM_{8LLE}	6	- 0.265 962 (201)	1×10^8	80
ΔM_{8LLF}	12	- 0.764 679 (413)		
<i>d-part</i>		- 0.618 362 (346)	2×10^8	80
<i>q-part1</i>		- 0.142 801 (221)	2×10^7	120
<i>q-part2</i>		- 0.003 516 (36)	1×10^6	400
ΔM_{8LLG}	12	- 0.550 968 (670)	4×10^8	80
ΔM_{8LLH}	6	0.190 770 (682)		
<i>d-part</i>		0.069 275 (379)	2×10^8	100
<i>q-part</i>		0.121 495 (566)	2×10^7	100
ΔM_{8LLI}	12	0.808 638 (482)	4×10^8	80

In most cases the first step is to make the integrand smoother by *stretching* (see Appendix B of Ref. [30]), which is repeated several times until the integrand behaves more gently.

Although *chopping* (see Appendix B of Ref. [30]) was handy to obtain a rough estimate quickly, we had to abandon it in the end because extrapolation to $\delta = 0$ turned out to be too unreliable in order to reach the desired precision.

Most integrals were then evaluated by *splitting* them into two parts, one evaluated in real*8 and the other in real*16. In some cases, however, even the part evaluated in real*16 suffered from severe *d-d* problem, preventing us from collecting large enough samplings for high statistics. Analyzing this problem closely, we found that it is possible to evaluate these integrals by the following procedure: First try several iterations with a positive rescale parameter β (typically $\beta = 0.5$) until VEGAS begins to show sign of blowing up due to the *d-d* problem. Then *freeze* β to 0 (see Appendix B of Ref. [30]). This may solve the problem in most cases. If not, try several iterations and see how rapidly the calculation runs into the *d-d* problem. It turns out that it takes place very early if we chose too many sampling points N_S per iteration. This is because choosing large N_S increases the chance of hitting random numbers too close to the singularity within one iteration. As a consequence the *d-d* problem is likely to dominate each iteration and makes it very difficult to collect large enough number of good samplings. A better strategy would be to reduce the size of N_S to a moderate value and, instead, increase the number of iterations N_I substantially. This is acceptable since, for $\beta = 0$ which means that the distribution function ρ is no longer changed from iteration to iteration, the final error generated by VEGAS depends only on the product $N_S N_I$.

This strategy has been applied in particular to the diagrams LLA and LLC, as is seen from Table VII. Entries in Table VII are only the best of results obtained by various methods discussed above. They are consistent with each other despite their diverse approaches.

One obtains from Table VII the *Version A* contributions of subgroups IV(b) and IV(c):

$$\begin{aligned} a_{IV(b)}^{(8)} &= 0.821\ 79\ (83), \\ a_{IV(c)}^{(8)} &= -1.138\ 71\ (117). \end{aligned} \tag{47}$$

B. Version B

In *Version B* the magnetic moment projection is evaluated for each vertex diagram on the LHS of (6). It is convenient to denote these diagrams in terms of self-energy-like diagrams

of Fig. 7, by attaching suffix i to indicate the lepton line in which an external magnetic field vertex is inserted. For instance, we obtain vertex diagrams LLA1, LLA2, ..., LLA5 from the diagram LLA.

We will not discuss subgroup IV(a) here since its *Version A* has already been fully tested. For subgroup IV(b) we find

$$a_{IV(b)}^{(8)} = \sum_{\alpha=A}^D \sum_{i=1}^5 \Delta M_{8LL\alpha i} - 4\Delta B_2 M_{6LL}, \quad (48)$$

instead of (45). Note that the last term of (48) is different from that of (45). This is not an error. It arises from difference in the definition of ΔM terms. Similarly, for subgroup IV(c) we obtain

$$a_{IV(c)}^{(8)} = \sum_{\alpha=E}^I \sum_{i=1}^3 \Delta M_{8LL\alpha i} - 2\Delta B_2 M_{6LL}. \quad (49)$$

Numerical evaluation of $\Delta M_{8LL\alpha i}$ are carried out with 10^9 sampling points per iteration. The results are listed in Table VIII. Precision of these calculations is somewhat higher than that of *Version A*. See the last column of Table VIII for comparison of two Versions. Although the values of ΔM_{8LLA} and ΔM_{8LLC} in two versions differ by several s. d., this is due to the influence of d - d problem. The general agreement between *Version A* and *Version B* leaves no doubt that their codes are free from any error.

One obtains from Table VIII the values of $a_{IV(b)}^{(8)}$ and $a_{IV(c)}^{(8)}$

$$\begin{aligned} a_{IV(b)}^{(8)} &= 0.822\ 57\ (30), \\ a_{IV(c)}^{(8)} &= -1.138\ 93\ (37), \end{aligned} \quad (50)$$

which are consistent with those given in (47).

C. Total contribution of Group IV

The contribution of subgroup IV(a) is listed only in (47) since it was not evaluated in *Version B*. Previously only subgroup IV(d) was evaluated in both versions with comparable statistical weights [17]. Now that subgroups IV(b) and IV(c) have been evaluated in two independent ways, we may combine their results statistically. This leads to our best estimate

TABLE VIII: Contribution of Group IV(b) and Group IV(c) diagrams of Fig. 7 evaluated in *Version B*. Double precision is used for all calculations which are carried out on RSCC at RIKEN. Finite renormalization terms $\Delta B_2 M_{6LLi}, i = 1, 2, 3$, are needed for LLA and LLC, respectively, in order to compare them with the calculations in *Version A*. $M_{6LL(2+3)} \equiv M_{6LL2} + M_{6LL3}$ is obtained subtracting M_{6LL1} from the known value of $M_{6LL} (\equiv M_{6LL1} + M_{6LL2} + M_{6LL3})$ given in (42).

Integral	n_F	Value (Error)	Sampling per	No. of	Difference
		including n_F	iteration	iterations	<i>Ver.A</i> - <i>Ver.B</i>
ΔM_{8LLA}	10	0.171 789 (131)			-0.000 262 (320)
$\sum_{i=1}^5 \eta_A \Delta M_{8LLAi}$		-0.096 030 (128)	1×10^9	300	
$-\Delta B_2 M_{6LL2}$		0.267 819 (27)	1×10^9	100	
ΔM_{8LLB}	20	-1.296 748 (161)	1×10^9	350	+0.000 631 (507)
ΔM_{8LLC}	20	2.840 956 (196)			-0.000 927 (549)
$\sum_{i=1}^5 \eta_C \Delta M_{8LLCi}$		3.387 028 (194)	1×10^9	516	
$-\Delta B_2 M_{6LL(1+3)}$		-0.546 072 (27)	1×10^9		
ΔM_{8LLD}	10	-0.058 661 (72)	1×10^9	420	-0.000 229 (332)
ΔM_{8LLE}	6	-0.265 908 (84)	1×10^9	420	-0.000 054 (218)
ΔM_{8LLF}	12	-0.764 424 (213)	1×10^9	520	-0.000 255 (465)
ΔM_{8LLG}	12	-0.551 233 (148)	1×10^9	400	0.000 265 (686)
ΔM_{8LLH}	6	0.190 023 (111)	1×10^9	400	+0.000 747 (691)
ΔM_{8LLI}	12	0.809 122 (217)	1×10^9	520	-0.000 484 (529)

for the gauge-invariant subgroups of group IV:

$$\begin{aligned}
a_{IV(a)}^{(8)} &= 0.598\ 95\ (14), \\
a_{IV(b)}^{(8)} &= 0.822\ 49\ (28), \\
a_{IV(c)}^{(8)} &= -1.138\ 91\ (35), \\
a_{IV(d)}^{(8)} &= -0.990\ 72\ (10).
\end{aligned} \tag{51}$$

Summing up these terms one find that the contribution from all 180 diagrams of group IV is given by

$$a_{IV}^{(8)} = -0.708\ 19\ (48). \quad (52)$$

VII. GROUP V DIAGRAMS

There are 518 vertex diagrams without closed electron loops that contribute to Group V. We have treated them only in *Version A* thus far, in which these vertex diagrams are represented by 74 self-energy-like diagrams. Since some of them are time-reversal of others, the number of independent integrals is reduced to 47, which are shown in Figs. 8 and 9.

Carrying out momentum space integration analytically by SCOONSCHIP and, more recently, by FORM, we obtain the magnetic moment projection of the Ward-Takahashi-summed amplitude as an integral over Feynman-parametric space of the form

$$M_{8\alpha} = \frac{3!}{256} \int (dz) \left(\frac{E_0 + C_0}{3U^2V^3} + \frac{E_1 + C_1}{3U^3V^2} + \frac{E_2 + C_2}{3U^4V} + \frac{N_0 + Z_0}{U^2V^4} + \frac{N_1 + Z_1}{U^3V^3} + \frac{N_2 + Z_2}{U^4V^2} + \frac{N_3 + Z_3}{U^5V} \right), \quad (53)$$

where $\alpha = 1, \dots, 47$. E_0 through Z_3 are polynomials of scalar currents B_{ij} and A_i . See [22, 30] for notation and definition.

Standard subtractive renormalization relates the $M_{8\alpha}$ to the renormalized contribution by

$$a_V^{(8)} = \sum_{\alpha=01}^{47} a_{8\alpha}, \quad (54)$$

where

$$a_{8\alpha} = M_{8\alpha} - \text{renormalization terms}. \quad (55)$$

$M_{8\alpha}$ is the sum of n_F vertex diagrams where n_F is given in the second column of Tables IX, X, XI, and XII. For simplicity we denote these amplitudes as M_α instead of $M_{8\alpha}$ in the following. To avoid possible confusion with M_2, M_4, \dots , defined elsewhere, however, let us denote M_1, M_2, \dots, M_9 as $M_{01}, M_{02}, \dots, M_{09}$.

The two-step renormalization of eighth-order terms is in principle no more difficult than that of lower-order terms, except that it requires many more subtraction terms. UV and IR

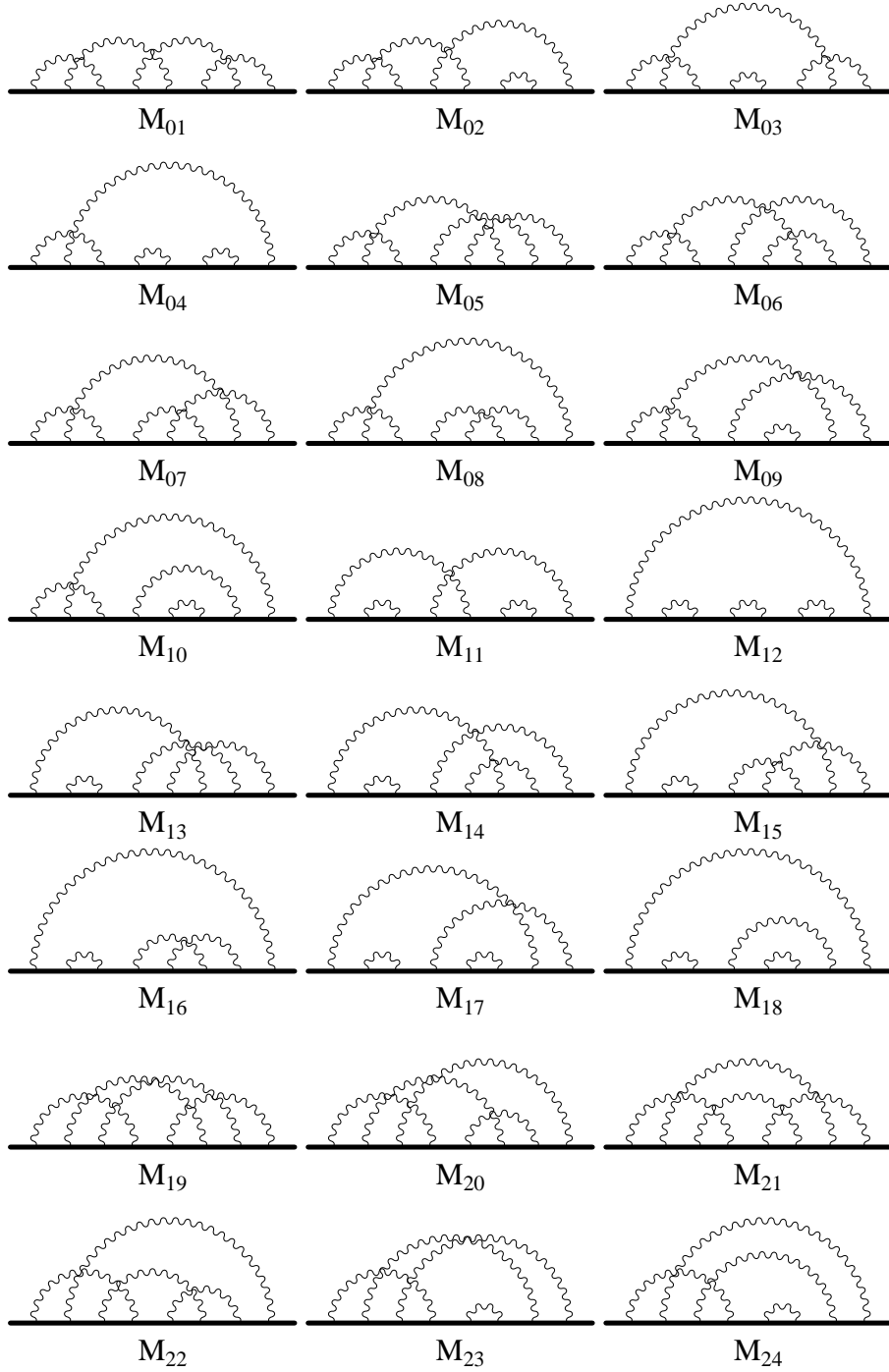


FIG. 8: Part of the electron self-energy-like diagrams M_{01} - M_{24} representing (external-vertex-summed) integrals of subgroup V.

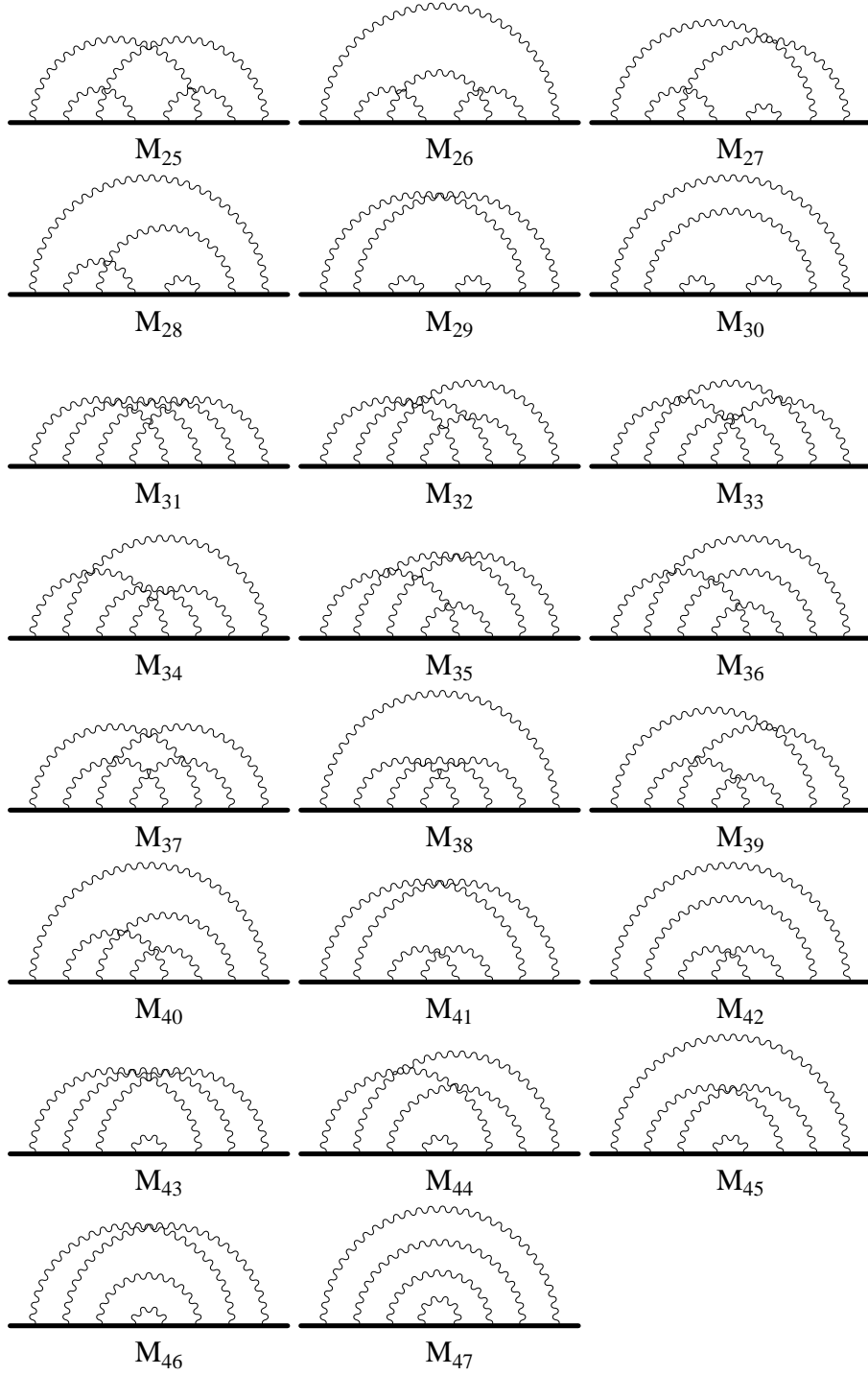


FIG. 9: Part of the electron self-energy-like diagrams M_{25} - M_{47} representing (external-vertex-summed) integrals of subgroup V.

subtraction terms of two-step renormalization scheme in *Version A* were originally derived manually. They were listed in Appendix D of Ref. [22]. In view of the fact that the two-step renormalization scheme plays the central role in the success of our numerical integration approach, we have re-examined its validity by a FORM program. The FORM program is then translated into LATEX format[47]. The result is listed in Appendix B together with the corresponding standard renormalization. We corrected some typographical errors in Ref. [22].

Collecting contributions of all terms of *Version A* we obtain

$$\begin{aligned}
a_V^{(8)} &= \Delta M^{(8)} - 5\Delta M^{(6)}\Delta B_2 \\
&- \Delta M^{(4)}[4\Delta L^{(4)} + 3\Delta B^{(4)} - 9(\Delta B_2)^2] - \Delta M^{(4*)}\Delta\delta m^{(4)} \\
&- M_2[2\Delta L^{(6)} + \Delta B^{(6)} - \Delta\delta m^{(4)}(4\Delta L_{2*} + \Delta B_{2*} - B_{2*}[I])] \\
&- (M_{2*} - M_{2*}[I])[\Delta\delta m^{(6)} - \Delta\delta m^{(4)}(5\Delta B_2 + \Delta\delta m_{2*})] \\
&+ M_2\Delta B_2[10\Delta L^{(4)} + 6\Delta B^{(4)} - 5(\Delta B_2)^2],
\end{aligned} \tag{56}$$

where (see Ref. [22] for notation)

$$\begin{aligned}
\Delta M^{(8)} &= \sum_{i=01}^{47} \Delta M_i, & \Delta M^{(6)} &= \sum_{\alpha=A}^H \Delta M_{6\alpha}, \\
\Delta M^{(4*)} &= 2\Delta M_{4a(1*)} + \Delta M_{4a(2*)} + 2\Delta M_{4b(1*)} + \Delta M_{4b(2*)}, \\
\Delta L^{(6)} &= \sum_{\alpha=A}^H \sum_{i=1}^5 \eta_\alpha \Delta L_{6\alpha i}, & \Delta B^{(6)} &= \sum_{\alpha=A}^H \eta_\alpha \Delta B_{6\alpha}, \\
\Delta\delta m^{(6)} &= \sum_{\alpha=A}^H \eta_\alpha \Delta\delta m_{6\alpha},
\end{aligned} \tag{57}$$

where ΔM_i represents the contribution of n_F vertices. $\Delta M_{6\alpha}$ is also the sum of several vertex diagrams. Meanwhile, η_α in front of $\Delta L_{6\alpha i}$, $\Delta B_{6\alpha}$, and $\Delta\delta m_{6\alpha}$ is their multiplicity.

Numerical evaluation of Group V integrals has been carried out by VEGAS. Tables IX, X, XI, and XII list only the latest of long sequence of work carried out over more than 17 years. Each integral was evaluated 5 to 10 times, starting with a relatively small number (typically $\sim 10^7$) of sampling points N_S , increasing it gradually to more than 10^9 as more and more computing power became available. Although these early data are not included in the final statistics, they have played important roles in providing consistency check among different runs. In several cases two statistically independent runs of similar high precision have been combined statistically, as is indicated in the Tables.

It was seldom that VEGAS gave good result in the first try. In most cases we had to search for alternate approach and/or transform the integrand by various means, such as remapping, higher precision arithmetic, stretching, splitting, freezing, and their combinations. (See Appendix B of Ref. [30] for terminology.)

As is seen from Tables IX - XII, only ten integrals gave good results with real*8 algebra. The remaining 37 diagrams required real*16 in some ways. In most cases *splitting* worked reasonably well. Integrals M_{04} , M_{16} , M_{18} , M_{26} , M_{28} , M_{30} , M_{42} , and M_{47} were evaluated in real*16 without relying on splitting. M_{04} , M_{16} , and M_{18} were evaluated also in the adjustable precision [48].

Evaluation of M_{40} in real*16 ran into a rather puzzling problem: For relatively small values of N_S this integral seemed to behave reasonably well. As we increased N_S , however, the error did not decrease as expected. For larger values of N_S , say $N_S \sim 10^9$, for which each iteration now has small enough error bars, several independent sequences of runs gave results which are different from each other by much more than the error estimates generated by VEGAS. We suspected that this was caused by a particularly severe *d-d* problem which made it difficult to choose a reasonable mapping. To pinpoint the cause of this annoying problem we decided to run M_{40} using real*32 arithmetic, which would reduce the *d-d* problem to a negligible level. Running M_{40} with $N_S = 8 \times 10^9$ so that intrinsic resolution of individual iteration generated by VEGAS is ~ 0.003 , we discovered that this integral fluctuates between two peaks which are far apart (~ 0.04) from each other. Once we discovered this problem, we went back to the beginning and chose a different mapping which does not have the double-peaking problem. Afterwards M_{40} behaved reasonably well. The value of M_{40} in Table XII was obtained entirely in real*32.

In comparison with M_{40} other diagrams were less troublesome in finding a reasonable mapping. However, diagram M_{12} showed sign of considerable *d-d* problem. We therefore evaluated M_{12} in real*32, too. The result is listed in Table IX.

Combining the data from Tables IX, X, XI, and XII as well as auxiliary integrals defined in (57) and listed in Table XIII, one can evaluate $a_V^{(8)}$ from (56). This leads to

$$a_V^{(8)} = -1.993\ 06\ (343). \tag{58}$$

The precision we have reported here is more than adequate for comparison with experiment for the time being. However, to prepare for the confrontation with future measurements

of a_e , further improvement of precision of some diagrams would be highly desirable.

Acknowledgments

The part of material presented by T. K. is based on work supported by the National Science Foundation under Grant No. PHY-0098631. M. N. is supported by the Ministry of Education, Science, Sports, and Culture, Grant-in-Aid for Scientific Research (c), 15540303. T. K. thanks the Eminent Scientist Invitation Program of RIKEN, Japan, for the hospitality extended to him where a part of this work was carried out. Thanks are due to J. Zollweg and R. Sinkovits for assistance in various phases of computation.

The numerical work has been carried out over more than 17 years on a number of computers. A part of work was conducted at the Cornell Theory Center using the resources of the Cornell University, New York State, the National Center for Research Resources of the National Institute of Health, the National Science Foundation, the Defense Department Modernization Program, the United States Department of Agriculture, and the corporate partners. Another part of numerical work was supported by NSF Cooperative agreement ACI-9619020 through computing resources provided by the National Partnership for Advanced Computational Infrastructure at the San Diego Super Computer Center, which enabled us to have an access to the Blue Horizon at the San Diego Supercomputer Center, the IBM SP at the University of Michigan, and the Condor Flock at the University of Wisconsin. M. N. thanks various computational resources provided by the Computer Center of Nara Women's University, RIKEN Super Computer System, and Matsuo Foundation.

APPENDIX A: ELIMINATION OF ALGEBRAIC ERROR OF GROUP V

The number of independent integrals of Group V is 47 in *Version A*. They are denoted as $M_{01}, M_{02}, \dots, M_{47}$ [22]. All integrals of Group V diagrams can be constructed from just one “template” by permutation of tensor indices of photons. This implies that any error in one of the integrals will propagate to other integrals. On the other hand, verification of one integral will verify all other integrals of Group V. All integrands are created by the following procedures:

TABLE IX: Contributions of diagrams $M_{01} - M_{13}$ of Fig. 8. Some integrals are split into two parts: d -part is evaluated in real*8 and q -part is evaluated in real*16. a -part refers to the adjustable precision method developed by [48]. The superscript “a” means that the adjustable precision method is used in the whole domain. The superscript “q-d” on ΔM_{12} indicates that it is run with real*32. Integrals without such qualification are evaluated in double precision. Only the latest results are listed. ΔM_{04} is a combination of two independent computations with comparable statistical weights.

Integral	n_F	Value (Error) including n_F	Sampling per iteration	No. of iterations
ΔM_{01}	7	- 0.216 765 (522)		
<i>d-part</i>		- 0.263 113 (397)	8×10^9	139
<i>q-part</i>		0.046 348 (338)	2×10^8	226
ΔM_{02}	14	- 0.274 402 (573)		
<i>d-part</i>		- 0.223 509 (347)	8×10^9	464
<i>q-part</i>		- 0.050 893 (455)	2×10^8	320
ΔM_{03}	7	- 0.681 633 (518)		
<i>d-part</i>		- 0.601 353 (358)	6×10^9	332
<i>q-part</i>		- 0.080 280 (374)	2×10^8	143
$\Delta M_{04}^{(a,q)}$	14	4.560 949 (838)	$3.5 \times 10^9, 4 \times 10^9$	233,209
ΔM_{05}	14	2.397 618 (266)	4×10^9	296
ΔM_{06}	14	- 1.447 248 (256)	4×10^9	286
ΔM_{07}	14	0.065 257 (282)	4×10^9	279
ΔM_{08}	14	- 6.576 977 (472)		
<i>d-part</i>		- 6.724 530 (343)	1.6×10^{10}	391
<i>q-part</i>		0.147 554 (323)	3×10^8	125
ΔM_{09}	14	0.937 503 (447)	8×10^9	409
ΔM_{10}	14	17.859 588 (600)		
<i>d-part</i>		16.823 753 (495)	2×10^{10}	403
<i>q-part</i>		1.035 835 (338)	4×10^8	189
ΔM_{11}	7	2.433 695 (336)		
<i>d-part</i>		2.372 864 (168)	1×10^{10}	378
<i>q-part</i>		0.060 831 (291)	1×10^8	100
$\Delta M_{12}^{(q-d)}$	7	- 4.096 653 (871)	1×10^9	316

TABLE X: Contributions of $M_{14} - M_{24}$ of Fig. 8. See the caption of Table IX for notation. Only latest results are listed. ΔM_{18} and $q - part_1$ of ΔM_{16} are statistical combinations of two independent runs.

Integral	n_F	Value (Error) including n_F	Sampling per iteration	No. of iterations
ΔM_{13}	14	- 6.658 475 (277)	8×10^9	280
ΔM_{14}	14	2.681 266 (404)		
<i>d-part</i>		2.653 346 (289)	7×10^9	269
<i>q-part</i>		0.027 920 (282)	2×10^8	114
ΔM_{15}	14	1.100 419 (473)		
<i>d-part</i>		1.199 683 (298)	5×10^9	237
<i>q-part</i>		- 0.099 264 (367)	2×10^8	236
ΔM_{16}	14	2.972 899 (758)		
<i>q - part₁</i>		2.821 674 (680)	$1 \times 10^{10}, 2 \times 10^9$	150,799
<i>q - part₂</i>		0.151 225 (334)	4×10^8	536
ΔM_{17}	14	3.157 998 (415)		
<i>d-part</i>		3.042 688 (253)	2.4×10^{10}	189
<i>q-part</i>		0.115 310 (329)	1.2×10^8	326
$\Delta M_{18}^{(a,q)}$	14	12.705 790 (695)	$4 \times 10^9, 4 \times 10^9$	188,145
ΔM_{19}	7	- 0.834 502 (266)		
<i>d-part</i>		- 0.753 570 (170)	4×10^8	221
<i>q-part</i>		- 0.080 932 (204)	2×10^7	99
ΔM_{20}	14	0.689 701 (320)		
<i>d-part</i>		0.604 560 (299)	1×10^9	102
<i>q-part</i>		0.085 141 (113)	2×10^7	105
ΔM_{21}	7	0.209 216 (281)		
<i>d-part</i>		0.191 592 (245)	4×10^8	99
<i>q-part</i>		0.017 624 (137)	2×10^7	100
ΔM_{22}	14	- 0.281 374 (454)		
<i>d-part</i>		- 0.226 185 (410)	1×10^9	110
<i>q-part</i>		- 0.055 189 (194)	2×10^7	100
ΔM_{23}	14	- 4.431 906 (473)		
<i>d-part</i>		- 4.139 207 (389)	3×10^9	289
<i>q-part</i>		- 0.292 699 (268)	4×10^7	80

TABLE XI: Contributions of diagrams $M_{25} - M_{39}$ of Fig. 9. See the caption of Table IX for notation. Only the latest results are listed.

Integral	n_F	Value (Error) including n_F	Sampling per iteration	No. of iterations
ΔM_{24}	14	2.206 446 (404)		
<i>d-part</i>		2.066 148 (263)	8×10^9	209
<i>q-part</i>		0.140 276 (314)	2×10^8	193
ΔM_{25}	7	0.080 642 (432)		
<i>a-part</i>		0.047 651 (167)	1×10^9	100
<i>a-part</i>		0.032 991 (398)	4×10^7	106
$\Delta M_{26}^{(q)}$	7	1.829 535 (545)	$9 \times 10^8, 1 \times 10^9$	173,222
ΔM_{27}	14	0.988 319 (383)		
<i>d-part</i>		0.838 417 (256)	4×10^9	145
<i>a-part</i>		0.149 902 (285)	1.2×10^8	311
$\Delta M_{28}^{(q,q)}$	14	- 4.950 479 (690)	$2.6 \times 10^9, 4 \times 10^9$	343,289
ΔM_{29}	7	3.083 789 (245)		
<i>d-part</i>		3.023 232 (130)	6×10^9	339
<i>a-part</i>		0.060 557 (207)	4×10^7	234
$\Delta M_{30}^{(q)}$	7	- 3.721 347 (630)	$2 \times 10^9, 2 \times 10^9$	159,206
ΔM_{31}	7	3.012 077 (179)	2×10^9	290
ΔM_{32}	14	- 2.377 888 (323)		
<i>d-part</i>		- 2.343 943 (284)	4×10^8	100
<i>a-part</i>		- 0.033 945 (153)	2×10^7	100
ΔM_{33}	7	- 1.194 130 (250)		
<i>d-part</i>		- 1.247 252 (243)	4×10^8	98
<i>q-part</i>		0.053 122 (57)	2×10^7	52
ΔM_{34}	14	1.341 091 (299)		
<i>d-part</i>		1.237 527 (149)	5×10^9	411
<i>q-part</i>		0.103 564 (259)	4×10^7	80
ΔM_{35}	14	- 0.539 732 (384)		
<i>d-part</i>		- 0.560 805 (376)	1×10^9	100
<i>q-part</i>		0.021 073 (75)	2×10^7	100
ΔM_{36}	14	- 0.302 434 (240)		
<i>d-part</i>		- 0.252 129 (113)	2×10^{10}	275
<i>q-part</i>		- 0.050 305 (211)	4×10^7	101

TABLE XII: Contributions of diagrams $M_{40} - M_{47}$ of Fig. 9. See the caption of Table IX for notation. The superscript “q-d” on ΔM_{40} indicates that it is run with real*32. Only the latest results are listed.

Integral	n_F	Value (Error) including n_F	Sampling per iteration	No. of iterations
ΔM_{37}	7	0.487 701 (305)	4×10^8	90
ΔM_{38}	7	- 3.094 936 (311)	8×10^9	147
ΔM_{39}	14	- 0.660 746 (290)	4×10^9	115
$\Delta M_{40}^{(q-d)}$	14	5.252 164 (977)	1×10^9	235
ΔM_{41}	7	- 1.416 949 (376)		
<i>d-part</i>		- 1.107 727 (256)	6×10^9	129
<i>q-part</i>		- 0.309 222 (275)	1.5×10^8	245
$\Delta M_{42}^{(q)}$	7	- 4.859 600 (678)	$2 \times 10^9, 2 \times 10^9$	168,226
ΔM_{43}	7	- 2.385 383 (221)	1×10^9	431
ΔM_{44}	14	3.468 870 (249)		
<i>d-part</i>		3.288 775 (78)	2×10^{10}	441
<i>q-part</i>		0.180 091 (236)	3×10^8	232
ΔM_{45}	7	0.711 911 (411)		
<i>d-part</i>		1.427 913 (217)	4×10^9	351
<i>q-part</i>		- 0.716 002 (349)	3×10^8	179
ΔM_{46}	7	- 6.766 038 (242)		
<i>d-part</i>		- 6.121 804 (86)	3×10^{10}	216
<i>q-part</i>		- 0.644 234 (226)	6×10^7	130
$\Delta M_{47}^{(q)}$	7	8.352 501 (585)	$2.4 \times 10^9, 2 \times 10^9$	205,179

a. Momentum-space integration is carried out analytically by an algebraic manipulation program FORM [15]. The result is expressed in terms of symbols A_i and B_{ij} (called *scalar currents* [22] because they obey an analogue of Kirchhoff’s laws for electric current in which Feynman parameters play the role of resistance [49]).

b. Diagrams of Group V belong to five *topologically distinct types* [22]. Correspondingly, scalar currents A_i and B_{ij} can be written explicitly as rational functions of Feynman parameters using one of the five “templates” for B_{ij} . Scalar currents must satisfy eight junction laws and four loop laws for each diagram. This imposes a very strict constraint on scalar

TABLE XIII: Auxiliary integrals for Group V. In this table we denote $\Delta M_{4a^*} \equiv 2\Delta M_{4a(1^*)} + \Delta M_{4a(2^*)}$. Similarly for ΔM_{4b^*} . $A_{LBD} \equiv \sum_{i=1}^5 \Delta L_{6Ai} + \frac{1}{2}\Delta B_{6A} + 2\Delta\delta m_{6A}$. Similarly for B_{LBD} , etc.

Integral	Value (Error)	Integral	Value (Error)
ΔB_{2^*}	1.5	ΔL_{2^*}	-0.75
$B_{2^*}[I]$	-0.5	$\Delta\delta m_{2^*}$	-0.75
ΔM_{4a^*}	3.636 02 (11)	ΔM_{4b^*}	10.147 24 (14)
ΔL_4	0.465 024 (17)	ΔB_4	-0.437 094 (21)
A_{LBD}	1.370 25 (52)	B_{LBD}	3.571 37 (26)
C_{LBD}	-6.778 82 (39)	$2 \times D_{LBD}$	-8.783 15 (40)
E_{LBD}	-1.592 21 (26)	F_{LBD}	2.652 93 (36)
$2 \times G_{LBD}$	3.890 15 (33)	H_{LBD}	-0.232 26 (13)
$\Delta M^{(6)}$	4.471 013 (45)		

currents and provides powerful defense against trivial programming errors.

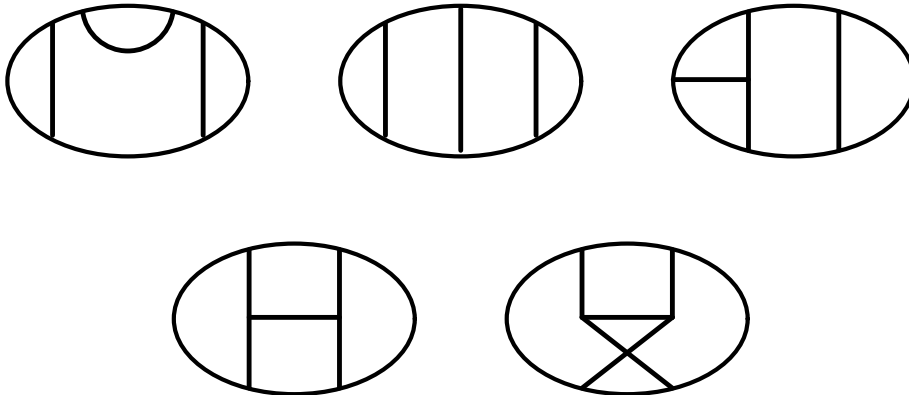


FIG. 10: Chain diagrams obtained from eighth-order diagrams by omitting external lines and disregarding the distinction between electron and photon lines. The topological structure of chain diagram is crucial for determining the structure of “scalar currents”.

c. Feynman-parametric integrals thus obtained are ultraviolet (UV) and/or infrared (IR) divergent in general. By a power counting rule designed for each divergence we can identify term by term which one is divergent [22]. Collection of these terms (in which only leading

terms are kept within each scalar current) forms a term required for renormalization. Its structure can be examined analytically by comparison with a known lower-order expression which is written as a Feynman-parametric integral over a function of *its own scalar currents*. These two integrals have different forms in general and their identity can be established only after some non-trivial analytic transformation. Comparison of these integrals provides an extremely powerful check of the subtraction term as well as major parts of mother integrand.

d. The only remaining task is to show that scalar currents themselves have no error. This is not difficult since the number of scalar currents is not large. This is the primary reason for expressing the integrand in terms of scalar currents instead of Feynman parameters themselves.

Initially, scalar currents were built by hands by two people working independently [21]. Comparison of resulting integrands enabled us to weed out human errors quickly. Recently we wrote programs in FORM (and MAPLE) which generate B_{ij} for each chain diagrams of Fig. 10 and show further that they satisfy all loop laws and junction laws.

Around 1992 we re-derived the entire integrands by a computer program in a form different from the original version. In this manner we obtained two sets of integrands with different algebraic structures. Their equivalence was checked by numerical *spot check*. This process was repeated for each renormalization term. Of course this comparison does not establish the validity of all terms. Since each diagram has several subtraction terms (as many as 20 in some cases), however, checks repeated for all subtraction terms cover a much larger fraction of the integrand than that of a single subtraction term and enhance strongly the confidence in the validity of the entire code.

The procedure outlined above is especially potent for the diagrams that contain a second-order electron self-energy part. When the integrand is expressed as a function of scalar currents, individual terms of the integrand, except those that contain the Feynman parameter z_{se} for the electron of the self-energy part explicitly, are UV divergent. This means that the corresponding self-energy subtraction term, *when expressed in terms of its own scalar currents*, has a form identical with that of the *mother integrand minus* terms proportional to z_{se} . Their difference comes solely from different structure of scalar currents for the mother and daughter integrands.

This argument applies equally well to diagrams which contain two second-order electron

self-energy parts. In this case *all* terms of the mother integrand can be verified by applying the above argument to each self-energy part, verifying the correctness of the template completely and thus all integrands obtained using the same template, namely, the entire Group V diagrams. In this manner we were able to confirm the validity of all terms of Group V integrals of *Version A*. Our very tight scheme *a.*, *b.*, *c.*, and *d* leaves no room for further algebraic error.

APPENDIX B: TWO-STEP RENORMALIZATION OF GROUP V INTEGRALS

Following the discussion in Refs.[12, 13, 22], we adopted the two-step renormalization scheme in the numerical evaluation of $g-2$. The **K** operation defined in Refs.[12, 22] picks up only the overall UV divergent part of the on-shell renormalization constant. It is used as the UV subtraction term in numerical calculation. The rest of the renormalization constants are combined in the end with those of other diagrams, which gives a finite contribution, referred to as the residual renormalization. The standard on-shell renormalization is the sum of **K** operation and residual renormalization. Only the renormalization scheme of *Version A* is given here since Group V has not been treated in *Version B*.

1. Renormalization Scheme for Group V

The eighth-order Group V diagrams have very complicated divergence structure. Only the **K** operation part was listed in Ref. [22] because of page restriction. For convenience of access and completeness we list here **K**-renormalization and standard renormalization together. Few typographic errors in the previous version are corrected.

We first list the standard on-shell renormalized amplitude a_i expressed in terms of the unrenormalized integral M_i and various renormalizing terms and then present the intermediate renormalization scheme which describes the relation between M_i and ΔM_i , the finite part of M_i defined by **K** operation. Substitution of M_i from the second part into the equation for a_i expresses it in terms of ΔM_i and pieces of renormalization constants as well as (unrenormalized) amplitudes of lower orders. Plugging them in (54) and using relations among lower order terms given in Appendix B2 we obtain Eq.(56).

M_{na} is the unrenormalized amplitude of the n th-order diagram a , where $n \leq 6$. A quantity

with prefactor Δ implies that it is finite. The infrared subtraction terms are denoted as I_{na} .

Quantities L_n , B_n , and δm_n denote vertex renormalization constant, wave-function renormalization constant, and mass renormalization constant of the n th-order, of the standard on-shell renormalization, respectively. In our approach by numerical integration, they are expressed as integrals over $3n$, $3n - 1$, and $3n - 1$ Feynman parameters, which enable us to perform cancellation of divergence at every point in the domain of integration. In the parametric form the divergent terms of an integrand can be readily identified by means of a power counting rule for each divergence. The sum of these terms are denoted as \hat{L}_n , \hat{B}_n , and $\delta\hat{m}_n$, and the remainder as \tilde{L}_n , etc. For instance, $L_2 = \hat{L}_2 + \tilde{L}_2$, where \hat{L}_2 is UV-divergent part picked up by the **K** operation and \tilde{L}_2 is the residual UV-finite term.

Within each subdiagram the electron lines are assumed to be consecutively labeled as $[1, 2, \dots, n_m]$, where $n_m = 2n$ for L_n and $2n - 1$ for B_n and δm_n , and the line 1 is at the tip of the arrow attached to the electron line.

The additional suffix such as c in L_{4c} indicates that it comes from the so-called *corner* diagram. Here we stick to the notation introduced previously. See Ref. [22], p.235, Fig. 8. The suffix (3^*) means the insertion of two-point vertex (such as mass-vertex) in the fermion line 3. The primed quantity $L_{4x(1')}$ is the derivative amplitude obtained by applying $-z_1 \frac{\partial}{\partial z_1}$ operation on the integrand, where z_1 is the Feynman parameter assigned to the fermion line 1. Note that $L_{4x(1')}$ is equal to L_{4x} , but its UV-divergent part $\hat{L}_{4x(1')}$ is not equal to \hat{L}_{4x} . Since second order quantities such as B_2 and δm_2 have only one electron line, it is not really necessary to distinguish different electron lines. We therefore use somewhat sloppy notations B_{2^*} and $B_{2'}$ instead of $B_{2(1^*)}$ and $B_{2(1')}$. Similarly, double insertions of two-point vertices are denoted as $B_{2^{**}}$, $B_{2'^*}$, $B_{2''}$, etc. Since δm_2 has no UV-finite part, $\delta\hat{m}_2$ is replaced by δm_2 everywhere. For L_2 , which contains electron lines 1 and 2, it is sometimes necessary to distinguish lines in which insertion is made. $L_{2^{**\dagger}}$ implies that two two-point vertices are inserted into the fermion line 1 of L_2 , while $L_{2^{\dagger**}}$ means that one two-point vertex is inserted into the line 1 and another into the line 2. M_{4a} contains three electron lines 1,2,3 and $M_{4a(1^{**})}$ means that two-point vertex insertion has been made twice in the electron line 1, and so on.

The validity of all equations has been confirmed algebraically by FORM. They are then

translated into LATEX format listed below [47].

On-Shell Renormalization for the Eighth-order Moments

$$a_{01} = M_{01} - 2M_{6F}L_2 - 2L_{6F1}M_2 - 2L_{4c}M_{4a} + 6L_{4c}L_2M_2 \\ + 3M_{4a}(L_2)^2 - 4(L_2)^3M_2$$

$$a_{02} = M_{02} - M_{6D}L_2 - M_{6F}B_2 - M_{6F(1^*)}\delta m_2 - L_{6D5}M_2 \\ + L_{4c(3^*)}\delta m_2M_2 - L_{4c}M_{4b} + L_{4c}\delta m_2M_{2^*} + 2L_{4c}B_2M_2 - L_{4s}M_{4a} \\ + 2L_{4s}L_2M_2 + M_{4a(1^*)}\delta m_2L_2 + M_{4b}(L_2)^2 + M_{4a}\delta m_2L_{2^*} + 2M_{4a}B_2L_2 \\ - 2\delta m_2L_2L_{2^*}M_2 - \delta m_2(L_2)^2M_{2^*} - 3B_2(L_2)^2M_2$$

$$a_{03} = M_{03} - 2M_{6D}L_2 - M_{6F}B_2 - M_{6F(3^*)}\delta m_2 - 2L_{6D1}M_2 \\ + 2L_{4c(1^*)}\delta m_2M_2 + 2L_{4c}B_2M_2 + 2L_{4s}L_2M_2 + 2M_{4a(1^*)}\delta m_2L_2 + M_{4b}(L_2)^2 \\ + 2M_{4a}B_2L_2 - 2\delta m_2L_2L_{2^*}M_2 - \delta m_2(L_2)^2M_{2^*} - 3B_2(L_2)^2M_2$$

$$a_{04} = M_{04} - M_{6A}L_2 - 2M_{6D}B_2 - M_{6D(1^*)}\delta m_2 - M_{6D(3^*)}\delta m_2 \\ - L_{6A1}M_2 + 2L_{4s(1^*)}\delta m_2M_2 + 2L_{4s}B_2M_2 + 2M_{4a(1^*)}\delta m_2B_2 + 2M_{4b(1^*)}\delta m_2L_2 \\ + 2M_{4b}B_2L_2 + M_{4a}(B_2)^2 + M_{4a(1^*1^*)}(\delta m_2)^2 - 2\delta m_2B_2L_2M_{2^*} - 2\delta m_2B_2L_{2^*}M_2 \\ - (\delta m_2)^2L_2M_{2^{**}} - (\delta m_2)^2L_{2^{**\dagger}}M_2 - 2(B_2)^2L_2M_2$$

$$a_{05} = M_{05} - M_{6H}L_2 - L_{6H1}M_2 - L_{6F2}M_2 - L_{4x}M_{4a} \\ + 3L_{4x}L_2M_2$$

$$a_{06} = M_{06} - M_{6F}L_2 - M_{6G}L_2 - L_{6F3}M_2 - L_{6G5}M_2 \\ + 3L_{4c}L_2M_2 - L_{4l}M_{4a} + 2L_{4l}L_2M_2 + 2M_{4a}(L_2)^2 - 3(L_2)^3M_2$$

$$a_{07} = M_{07} - M_{6F}L_2 - M_{6G}L_2 - L_{6G1}M_2 - L_{6D2}M_2 \\ - L_{4c}M_{4a} + 4L_{4c}L_2M_2 + L_{4l}L_2M_2 + 2M_{4a}(L_2)^2 - 3(L_2)^3M_2$$

$$\begin{aligned}
a_{08} = & M_{08} - M_{6C}L_2 - 2M_{6D}L_2 - L_{6C1}M_2 - \delta m_{4a}M_{4a(1^*)} \\
& + \delta m_{4a}L_2M_{2^*} + \delta m_{4a}L_{2^*}M_2 - B_{4a}M_{4a} + 2B_{4a}L_2M_2 + 2L_{4s}L_2M_2 \\
& + 2M_{4a(1^*)}\delta m_2L_2 + 2M_{4b}(L_2)^2 + 2M_{4a}B_2L_2 - 2\delta m_2L_2L_{2^*}M_2 - 2\delta m_2(L_2)^2M_{2^*} \\
& - 4B_2(L_2)^2M_2
\end{aligned}$$

$$\begin{aligned}
a_{09} = & M_{09} - M_{6E}L_2 - M_{6F}B_2 - M_{6F(2^*)}\delta m_2 - L_{6E1}M_2 \\
& - L_{6D3}M_2 + L_{4c(1^*)}\delta m_2M_2 + L_{4c(2^*)}\delta m_2M_2 + 2L_{4c}B_2M_2 - L_{4s}M_{4a} \\
& + 3L_{4s}L_2M_2 + M_{4a(2^*)}\delta m_2L_2 + M_{4a}\delta m_2L_{2^*} + 2M_{4a}B_2L_2 - 3\delta m_2L_2L_{2^*}M_2 \\
& - 3B_2(L_2)^2M_2
\end{aligned}$$

$$\begin{aligned}
a_{10} = & M_{10} - M_{6B}L_2 - M_{6D}B_2 - M_{6D(2^*)}\delta m_2 - L_{6B1}M_2 \\
& + L_{4s(2^*)}\delta m_2M_2 - \delta m_{4b}M_{4a(1^*)} + \delta m_{4b}L_2M_{2^*} + \delta m_{4b}L_{2^*}M_2 - B_{4b}M_{4a} \\
& + 2B_{4b}L_2M_2 + L_{4s}B_2M_2 + M_{4a(1^*)}\delta m_2\delta m_{2^*} + M_{4a(1^*)}\delta m_2B_2 + M_{4b(2^*)}\delta m_2L_2 \\
& + M_{4b}B_2L_2 + M_{4a}\delta m_2B_{2^*} + M_{4a}(B_2)^2 - \delta m_2\delta m_{2^*}L_2M_{2^*} - \delta m_2\delta m_{2^*}L_{2^*}M_2 \\
& - \delta m_2B_2L_2M_{2^*} - \delta m_2B_2L_{2^*}M_2 - 2\delta m_2B_{2^*}L_2M_2 - 2(B_2)^2L_2M_2
\end{aligned}$$

$$\begin{aligned}
a_{11} = & M_{11} - 2M_{6D}B_2 - 2M_{6D(5^*)}\delta m_2 - 2L_{4s}M_{4b} + 2L_{4s}\delta m_2M_{2^*} \\
& + 2L_{4s}B_2M_2 + 2M_{4a(1^*)}\delta m_2B_2 + 2M_{4b}\delta m_2L_{2^*} + 2M_{4b}B_2L_2 + M_{4a}(B_2)^2 \\
& + M_{4a(1^*3^*)}(\delta m_2)^2 - 2\delta m_2B_2L_2M_{2^*} - 2\delta m_2B_2L_{2^*}M_2 - 2(\delta m_2)^2L_{2^*}M_{2^*} - 2(B_2)^2L_2M_2
\end{aligned}$$

$$\begin{aligned}
a_{12} = & M_{12} - 3M_{6A}B_2 - 2M_{6A(1^*)}\delta m_2 - M_{6A(3^*)}\delta m_2 + 6M_{4b(1^*)}\delta m_2B_2 \\
& + 3M_{4b}(B_2)^2 + 2M_{4b(1^*1^*)}(\delta m_2)^2 + M_{4b(1^*3^*)}(\delta m_2)^2 - 3\delta m_2(B_2)^2M_{2^*} - 3(\delta m_2)^2B_2M_{2^{**}} \\
& - (\delta m_2)^3M_{2^{***}} - (B_2)^3M_2
\end{aligned}$$

$$\begin{aligned}
a_{13} = & M_{13} - M_{6H}B_2 - M_{6H(1^*)}\delta m_2 - L_{6D4}M_2 + L_{4x(1^*)}\delta m_2M_2 \\
& - L_{4x}M_{4b} + L_{4x}\delta m_2M_{2^*} + 2L_{4x}B_2M_2
\end{aligned}$$

$$\begin{aligned}
a_{14} = & M_{14} - M_{6D}L_2 - M_{6G}B_2 - M_{6G(5^*)}\delta m_2 - L_{6D3}M_2 \\
& + L_{4c(1^*)}\delta m_2M_2 + L_{4c}B_2M_2 + L_{4s}L_2M_2 - L_{4l}M_{4b} + L_{4l}\delta m_2M_{2^*} \\
& + L_{4l}B_2M_2 + M_{4a(1^*)}\delta m_2L_2 + M_{4b}(L_2)^2 + M_{4a}B_2L_2 - \delta m_2L_2L_{2^*}M_2 \\
& - \delta m_2(L_2)^2M_{2^*} - 2B_2(L_2)^2M_2
\end{aligned}$$

$$\begin{aligned}
a_{15} = & M_{15} - M_{6D}L_2 - M_{6G}B_2 - M_{6G(1^*)}\delta m_2 - L_{6A2}M_2 \\
& + L_{4l(1^*)}\delta m_2 M_2 - L_{4c}M_{4b} + L_{4c}\delta m_2 M_{2^*} + L_{4c}B_2 M_2 + L_{4s}L_2 M_2 \\
& + L_{4l}B_2 M_2 + M_{4a(1^*)}\delta m_2 L_2 + M_{4b}(L_2)^2 + M_{4a}B_2 L_2 - \delta m_2 L_2 L_{2^*} M_2 \\
& - \delta m_2 (L_2)^2 M_{2^*} - 2B_2 (L_2)^2 M_2
\end{aligned}$$

$$\begin{aligned}
a_{16} = & M_{16} - 2M_{6A}L_2 - M_{6C}B_2 - M_{6C(1^*)}\delta m_2 - \delta m_{4a}M_{4b(1^*)} \\
& + \delta m_{4a}\delta m_2 M_{2^{**}} + \delta m_{4a}B_2 M_{2^*} - B_{4a}M_{4b} + B_{4a}\delta m_2 M_{2^*} + B_{4a}B_2 M_2 \\
& + 4M_{4b(1^*)}\delta m_2 L_2 + 4M_{4b}B_2 L_2 - 4\delta m_2 B_2 L_2 M_{2^*} - 2(\delta m_2)^2 L_2 M_{2^{**}} - 2(B_2)^2 L_2 M_2
\end{aligned}$$

$$\begin{aligned}
a_{17} = & M_{17} - M_{6D}B_2 - M_{6E}B_2 - M_{6E(1^*)}\delta m_2 - M_{6D(4^*)}\delta m_2 \\
& - L_{6A3}M_2 + 2L_{4s(1^*)}\delta m_2 M_2 - L_{4s}M_{4b} + L_{4s}\delta m_2 M_{2^*} + 3L_{4s}B_2 M_2 \\
& + M_{4a(1^*)}\delta m_2 B_2 + M_{4a(2^*)}\delta m_2 B_2 + M_{4b}\delta m_2 L_{2^*} + M_{4b}B_2 L_2 + M_{4a}(B_2)^2 \\
& + M_{4a(1^*2^*)}(\delta m_2)^2 - \delta m_2 B_2 L_2 M_{2^*} - 3\delta m_2 B_2 L_{2^*} M_2 - (\delta m_2)^2 L_{2^*} M_{2^*} - (\delta m_2)^2 L_{2^* \dagger} M_2 \\
& - 2(B_2)^2 L_2 M_2
\end{aligned}$$

$$\begin{aligned}
a_{18} = & M_{18} - M_{6A}B_2 - M_{6B}B_2 - M_{6B(1^*)}\delta m_2 - M_{6A(2^*)}\delta m_2 \\
& - \delta m_{4b}M_{4b(1^*)} + \delta m_{4b}\delta m_2 M_{2^{**}} + \delta m_{4b}B_2 M_{2^*} - B_{4b}M_{4b} + B_{4b}\delta m_2 M_{2^*} \\
& + B_{4b}B_2 M_2 + M_{4b(1^*)}\delta m_2 \delta m_{2^*} + 2M_{4b(1^*)}\delta m_2 B_2 + M_{4b(2^*)}\delta m_2 B_2 + M_{4b}\delta m_2 B_{2^*} \\
& + 2M_{4b}(B_2)^2 + M_{4b(1^*2^*)}(\delta m_2)^2 - \delta m_2 \delta m_{2^*} B_2 M_{2^*} - \delta m_2 B_2 B_{2^*} M_2 - 2\delta m_2 (B_2)^2 M_{2^*} \\
& - (\delta m_2)^2 \delta m_{2^*} M_{2^{**}} - (\delta m_2)^2 B_2 M_{2^{**}} - (\delta m_2)^2 B_{2^*} M_{2^*} - (B_2)^3 M_2
\end{aligned}$$

$$a_{19} = M_{19} - 2L_{6H2}M_2$$

$$a_{20} = M_{20} - M_{6H}L_2 - L_{6F2}M_2 - L_{6G4}M_2 + 2L_{4x}L_2M_2$$

$$a_{21} = M_{21} - 2L_{6G2}M_2$$

$$\begin{aligned}
a_{22} = & M_{22} - M_{6G}L_2 - L_{6F1}M_2 - L_{6C2}M_2 - L_{4c}M_{4a} \\
& + 3L_{4c}L_2M_2 + L_{4l}L_2M_2 + M_{4a}(L_2)^2 - 2(L_2)^3M_2
\end{aligned}$$

$$a_{23} = M_{23} - M_{6H}B_2 - M_{6H(2^*)}\delta m_2 - L_{6E2}M_2 - L_{6D4}M_2 \\ + L_{4x(1^*)}\delta m_2M_2 + L_{4x(2^*)}\delta m_2M_2 + 2L_{4x}B_2M_2$$

$$a_{24} = M_{24} - M_{6G}B_2 - M_{6G(2^*)}\delta m_2 - L_{6B2}M_2 - L_{6D5}M_2 \\ + L_{4c(1^*)}\delta m_2M_2 + L_{4l(2^*)}\delta m_2M_2 + L_{4c}B_2M_2 - L_{4s}M_{4a} + 2L_{4s}L_2M_2 \\ + L_{4l}B_2M_2 + M_{4a}\delta m_2L_2^* + M_{4a}B_2L_2 - 2\delta m_2L_2L_2^*M_2 - 2B_2(L_2)^2M_2$$

$$a_{25} = M_{25} - 2M_{6G}L_2 - 2L_{6D2}M_2 + 2L_{4c}L_2M_2 + 2L_{4l}L_2M_2 \\ + M_{4a}(L_2)^2 - 2(L_2)^3M_2$$

$$a_{26} = M_{26} - 2M_{6C}L_2 - \delta m_{6F}M_2^* - B_{6F}M_2 + 2\delta m_{4a}L_2M_2^* \\ + 2B_{4a}L_2M_2 - 2L_{4c}M_{4b} + 2L_{4c}\delta m_2M_2^* + 2L_{4c}B_2M_2 + 3M_{4b}(L_2)^2 \\ - 3\delta m_2(L_2)^2M_2^* - 3B_2(L_2)^2M_2$$

$$a_{27} = M_{27} - M_{6E}L_2 - M_{6G}B_2 - M_{6G(4^*)}\delta m_2 - L_{6D1}M_2 \\ - L_{6A2}M_2 + L_{4c(1^*)}\delta m_2M_2 + L_{4l(1^*)}\delta m_2M_2 + L_{4c}B_2M_2 + 2L_{4s}L_2M_2 \\ + L_{4l}B_2M_2 + M_{4a(2^*)}\delta m_2L_2 + M_{4a}B_2L_2 - 2\delta m_2L_2L_2^*M_2 - 2B_2(L_2)^2M_2$$

$$a_{28} = M_{28} - M_{6B}L_2 - M_{6C}B_2 - M_{6C(2^*)}\delta m_2 - \delta m_{6D}M_2^* \\ - B_{6D}M_2 + \delta m_{4a(1^*)}\delta m_2M_2^* + B_{4a(1^*)}\delta m_2M_2 + \delta m_{4a}B_2M_2^* + \delta m_{4b}L_2M_2^* \\ + B_{4a}B_2M_2 + B_{4b}L_2M_2 - L_{4s}M_{4b} + L_{4s}\delta m_2M_2^* + L_{4s}B_2M_2 \\ + M_{4b(2^*)}\delta m_2L_2 + M_{4b}\delta m_2L_2^* + 2M_{4b}B_2L_2 - \delta m_2\delta m_2^*L_2M_2^* - 2\delta m_2B_2L_2M_2^* \\ - \delta m_2B_2L_2^*M_2 - \delta m_2B_2^*L_2M_2 - (\delta m_2)^2L_2^*M_2^* - 2(B_2)^2L_2M_2$$

$$a_{29} = M_{29} - 2M_{6E}B_2 - 2M_{6E(2^*)}\delta m_2 - 2L_{6A1}M_2 + 4L_{4s(1^*)}\delta m_2M_2 \\ + 4L_{4s}B_2M_2 + 2M_{4a(2^*)}\delta m_2B_2 + M_{4a}(B_2)^2 + M_{4a(2^*2^*)}(\delta m_2)^2 - 4\delta m_2B_2L_2^*M_2 \\ - 2(\delta m_2)^2L_2^{**\dagger}M_2 - 2(B_2)^2L_2M_2$$

$$a_{30} = M_{30} - 2M_{6B}B_2 - 2M_{6B(2^*)}\delta m_2 - \delta m_{6A}M_2^* - B_{6A}M_2 \\ + 2\delta m_{4b(1^*)}\delta m_2M_2^* + 2B_{4b(1^*)}\delta m_2M_2 + 2\delta m_{4b}B_2M_2^* + 2B_{4b}B_2M_2 + 2M_{4b(2^*)}\delta m_2B_2 \\ + M_{4b}(B_2)^2 + M_{4b(2^*2^*)}(\delta m_2)^2 - 2\delta m_2\delta m_2^*B_2M_2^* - 2\delta m_2B_2B_2^*M_2 - \delta m_2(B_2)^2M_2^* \\ - (\delta m_2)^2\delta m_2^{**}M_2^* - (\delta m_2)^2B_2^{**}M_2 - (B_2)^3M_2$$

$$a_{31} = M_{31} - 2L_{6H3}M_2$$

$$a_{32} = M_{32} - L_{6H2}M_2 - L_{6G3}M_2$$

$$a_{33} = M_{33} - 2L_{6G3}M_2$$

$$a_{34} = M_{34} - L_{6H1}M_2 - L_{6C3}M_2 - L_{4x}M_{4a} + 2L_{4x}L_2M_2$$

$$a_{35} = M_{35} - M_{6H}L_2 - L_{6E3}M_2 - L_{6G4}M_2 + 2L_{4x}L_2M_2$$

$$a_{36} = M_{36} - M_{6G}L_2 - L_{6B3}M_2 - L_{6G5}M_2 + L_{4c}L_2M_2 \\ - L_{4l}M_{4a} + 3L_{4l}L_2M_2 + M_{4a}(L_2)^2 - 2(L_2)^3M_2$$

$$a_{37} = M_{37} - 2L_{6G2}M_2$$

$$a_{38} = M_{38} - \delta m_{6H}M_{2^*} - B_{6H}M_2 - 2L_{4x}M_{4b} + 2L_{4x}\delta m_2M_{2^*} + 2L_{4x}B_2M_2$$

$$a_{39} = M_{39} - M_{6G}L_2 - L_{6G1}M_2 - L_{6C2}M_2 - L_{4c}M_{4a} \\ + 3L_{4c}L_2M_2 + L_{4l}L_2M_2 + M_{4a}(L_2)^2 - 2(L_2)^3M_2$$

$$a_{40} = M_{40} - M_{6C}L_2 - \delta m_{6G}M_{2^*} - B_{6G}M_2 + \delta m_{4a}L_2M_{2^*} \\ + B_{4a}L_2M_2 - L_{4c}M_{4b} + L_{4c}\delta m_2M_{2^*} + L_{4c}B_2M_2 - L_{4l}M_{4b} \\ + L_{4l}\delta m_2M_{2^*} + L_{4l}B_2M_2 + 2M_{4b}(L_2)^2 - 2\delta m_2(L_2)^2M_{2^*} - 2B_2(L_2)^2M_2$$

$$a_{41} = M_{41} - 2M_{6E}L_2 - 2L_{6C1}M_2 - \delta m_{4a}M_{4a(2^*)} + 2\delta m_{4a}L_{2^*}M_2 \\ - B_{4a}M_{4a} + 2B_{4a}L_2M_2 + 4L_{4s}L_2M_2 + 2M_{4a(2^*)}\delta m_2L_2 + 2M_{4a}B_2L_2 \\ - 4\delta m_2L_2L_{2^*}M_2 - 4B_2(L_2)^2M_2$$

$$a_{42} = M_{42} - 2M_{6B}L_2 - \delta m_{6C}M_{2^*} - B_{6C}M_2 - \delta m_{4a}M_{4b(2^*)} \\ + \delta m_{4a}\delta m_{2^*}M_{2^*} + \delta m_{4a}B_{2^*}M_2 + 2\delta m_{4b}L_2M_{2^*} - B_{4a}M_{4b} + B_{4a}\delta m_2M_{2^*} \\ + B_{4a}B_2M_2 + 2B_{4b}L_2M_2 + 2M_{4b(2^*)}\delta m_2L_2 + 2M_{4b}B_2L_2 - 2\delta m_2\delta m_{2^*}L_2M_{2^*} \\ - 2\delta m_2B_2L_2M_{2^*} - 2\delta m_2B_{2^*}L_2M_2 - 2(B_2)^2L_2M_2$$

$$a_{43} = M_{43} - M_{6H}B_2 - M_{6H(3^*)}\delta m_2 - 2L_{6E2}M_2 + 2L_{4x(2^*)}\delta m_2M_2 \\ + 2L_{4x}B_2M_2$$

$$a_{44} = M_{44} - M_{6G}B_2 - M_{6G(3^*)}\delta m_2 - L_{6E1}M_2 - L_{6B2}M_2 \\ + L_{4c(2^*)}\delta m_2M_2 + L_{4l(2^*)}\delta m_2M_2 + L_{4c}B_2M_2 - L_{4s}M_{4a} + 2L_{4s}L_2M_2 \\ + L_{4l}B_2M_2 + M_{4a}\delta m_2L_{2^*} + M_{4a}B_2L_2 - 2\delta m_2L_2L_{2^*}M_2 - 2B_2(L_2)^2M_2$$

$$a_{45} = M_{45} - M_{6C}B_2 - M_{6C(3^*)}\delta m_2 - \delta m_{6E}M_{2^*} - B_{6E}M_2 \\ + \delta m_{4a(2^*)}\delta m_2M_{2^*} + B_{4a(2^*)}\delta m_2M_2 + \delta m_{4a}B_2M_{2^*} + B_{4a}B_2M_2 - 2L_{4s}M_{4b} \\ + 2L_{4s}\delta m_2M_{2^*} + 2L_{4s}B_2M_2 + 2M_{4b}\delta m_2L_{2^*} + 2M_{4b}B_2L_2 - 2\delta m_2B_2L_2M_{2^*} \\ - 2\delta m_2B_2L_{2^*}M_2 - 2(\delta m_2)^2L_{2^*}M_{2^*} - 2(B_2)^2L_2M_2$$

$$a_{46} = M_{46} - M_{6E}B_2 - M_{6E(3^*)}\delta m_2 - 2L_{6B1}M_2 + 2L_{4s(2^*)}\delta m_2M_2 \\ - \delta m_{4b}M_{4a(2^*)} + 2\delta m_{4b}L_{2^*}M_2 - B_{4b}M_{4a} + 2B_{4b}L_2M_2 + 2L_{4s}B_2M_2 \\ + M_{4a(2^*)}\delta m_2\delta m_{2^*} + M_{4a(2^*)}\delta m_2B_2 + M_{4a}\delta m_2B_{2^*} + M_{4a}(B_2)^2 - 2\delta m_2\delta m_{2^*}L_{2^*}M_2 \\ - 2\delta m_2B_2L_{2^*}M_2 - 2\delta m_2B_{2^*}L_2M_2 - 2(B_2)^2L_2M_2$$

$$a_{47} = M_{47} - M_{6B}B_2 - M_{6B(3^*)}\delta m_2 - \delta m_{6B}M_{2^*} - B_{6B}M_2 \\ + \delta m_{4b(2^*)}\delta m_2M_{2^*} + B_{4b(2^*)}\delta m_2M_2 - \delta m_{4b}M_{4b(2^*)} + \delta m_{4b}\delta m_{2^*}M_{2^*} + \delta m_{4b}B_2M_{2^*} \\ + \delta m_{4b}B_{2^*}M_2 - B_{4b}M_{4b} + B_{4b}\delta m_2M_{2^*} + 2B_{4b}B_2M_2 + M_{4b(2^*)}\delta m_2\delta m_{2^*} \\ + M_{4b(2^*)}\delta m_2B_2 + M_{4b}\delta m_2B_{2^*} + M_{4b}(B_2)^2 - \delta m_2\delta m_{2^*}B_2M_{2^*} - \delta m_2\delta m_{2^*}B_{2^*}M_2 \\ - \delta m_2(\delta m_{2^*})^2M_{2^*} - 2\delta m_2B_2B_{2^*}M_2 - \delta m_2(B_2)^2M_{2^*} - (\delta m_2)^2B_{2^*}M_{2^*} - (B_2)^3M_2$$

Intermediate Renormalization for the Eighth-order Moments

$$M_{01} = \Delta M_{01} + 2M_{6F}\hat{L}_2 + 2\hat{L}_{6F1}M_2 + 2\hat{L}_{4c}M_{4a} - 6\hat{L}_{4c}\hat{L}_2M_2 \\ - 3M_{4a}(\hat{L}_2)^2 + 4(\hat{L}_2)^3M_2$$

$$\begin{aligned}
M_{02} &= \Delta M_{02} + M_{6D}\hat{L}_2 + M_{6F}\hat{B}_2 + M_{6F(1^*)}\delta m_2 + I_{6F1}M_2 \\
&+ \hat{L}_{6D5}M_2 + \hat{L}_{4c}M_{4b} - \hat{L}_{4c}\delta m_2 M_{2^*} - \hat{L}_{4c}\hat{B}_2 M_2 + \hat{L}_{4s}M_{4a} \\
&- 2\hat{L}_{4s}\hat{L}_2 M_2 - \hat{L}_{4c(3')}\hat{B}_2 M_2 + \Delta L_{4c}M_2 I_2 - M_{4a(1^*)}\delta m_2 \hat{L}_2 - M_{4b}(\hat{L}_2)^2 \\
&- M_{4a}\hat{B}_2 \hat{L}_2 - M_{4a}\hat{B}_2 \hat{L}_{2'} + \delta m_2 (\hat{L}_2)^2 M_{2^*} + 2\hat{B}_2 \hat{L}_2 M_2 \hat{L}_{2'} + \hat{B}_2 (\hat{L}_2)^2 M_2
\end{aligned}$$

$$\begin{aligned}
M_{03} &= \Delta M_{03} + 2M_{6D}\hat{L}_2 + M_{6F}\hat{B}_2 + M_{6F(3^*)}\delta m_2 + 2\hat{L}_{6D1}M_2 \\
&+ I_{6F3}M_2 - 2\hat{L}_{4s}\hat{L}_2 M_2 - 2\hat{L}_{4c((1')')}\hat{B}_2 M_2 - 2M_{4a(1^*)}\delta m_2 \hat{L}_2 - M_{4b}(\hat{L}_2)^2 \\
&- 2M_{4a}\hat{B}_2 \hat{L}_2 + \delta m_2 (\hat{L}_2)^2 M_{2^*} + 2\hat{B}_2 \hat{L}_2 M_2 \hat{L}_{2'} + \hat{B}_2 (\hat{L}_2)^2 M_2
\end{aligned}$$

$$\begin{aligned}
M_{04} &= \Delta M_{04} + M_{6A}\hat{L}_2 + 2M_{6D}\hat{B}_2 + M_{6D(1^*)}\delta m_2 + M_{6D(3^*)}\delta m_2 \\
&+ \hat{L}_{6A1}M_2 + I_{6D1}M_2 + I_{6D3}M_2 - \hat{L}_{4s((1')')}\hat{B}_2 M_2 - \hat{L}_{4s(3')}\hat{B}_2 M_2 \\
&- 2M_{4a(1^*)}\delta m_2 \hat{B}_2 - 2M_{4b(1^*)}\delta m_2 \hat{L}_2 - 2M_{4b}\hat{B}_2 \hat{L}_2 - M_{4a}(\hat{B}_2)^2 - M_{4a(1^*1^*)}(\delta m_2)^2 \\
&+ \hat{L}_{2'}(\hat{B}_2)^2 M_2 + 2\delta m_2 \hat{B}_2 \hat{L}_2 M_{2^*} + (\delta m_2)^2 \hat{L}_2 M_{2^{**}} + (\hat{B}_2)^2 \hat{L}_2 M_2
\end{aligned}$$

$$\begin{aligned}
M_{05} &= \Delta M_{05} + M_{6H}\hat{L}_2 + \hat{L}_{6H1}M_2 + \hat{L}_{6F2}M_2 + \hat{L}_{4x}M_{4a} \\
&- 3\hat{L}_{4x}\hat{L}_2 M_2
\end{aligned}$$

$$\begin{aligned}
M_{06} &= \Delta M_{06} + M_{6F}\hat{L}_2 + M_{6G}\hat{L}_2 + \hat{L}_{6F3}M_2 + \hat{L}_{6G5}M_2 \\
&- 3\hat{L}_{4c}\hat{L}_2 M_2 + \hat{L}_{4l}M_{4a} - 2\hat{L}_{4l}\hat{L}_2 M_2 - 2M_{4a}(\hat{L}_2)^2 + 3(\hat{L}_2)^3 M_2
\end{aligned}$$

$$\begin{aligned}
M_{07} &= \Delta M_{07} + M_{6F}\hat{L}_2 + M_{6G}\hat{L}_2 + \hat{L}_{6G1}M_2 + \hat{L}_{6D2}M_2 \\
&+ \hat{L}_{4c}M_{4a} - 4\hat{L}_{4c}\hat{L}_2 M_2 - \hat{L}_{4l}\hat{L}_2 M_2 - 2M_{4a}(\hat{L}_2)^2 + 3(\hat{L}_2)^3 M_2
\end{aligned}$$

$$\begin{aligned}
M_{08} &= \Delta M_{08} + M_{6C}\hat{L}_2 + 2M_{6D}\hat{L}_2 + \hat{L}_{6C1}M_2 + \delta \hat{m}_{4a}M_{4a(1^*)} \\
&- \delta \hat{m}_{4a}\hat{L}_2 M_{2^*} + \hat{B}_{4a}M_{4a} - \hat{B}_{4a}\hat{L}_2 M_2 - \hat{B}_{4a}M_2 \hat{L}_{2'} - 2\hat{L}_{4s}\hat{L}_2 M_2 \\
&+ \Delta \delta m_{4a}I_{4a(1^*)} - 2M_{4a(1^*)}\delta m_2 \hat{L}_2 - 2M_{4b}(\hat{L}_2)^2 - 2M_{4a}\hat{B}_2 \hat{L}_2 + \Delta M_{4a}I_{4c} \\
&+ 2\delta m_2 (\hat{L}_2)^2 M_{2^*} + 2\hat{B}_2 \hat{L}_2 M_2 \hat{L}_{2'} + 2\hat{B}_2 (\hat{L}_2)^2 M_2
\end{aligned}$$

$$\begin{aligned}
M_{09} &= \Delta M_{09} + M_{6E}\hat{L}_2 + M_{6F}\hat{B}_2 + M_{6F(2^*)}\delta m_2 + \hat{L}_{6E1}M_2 \\
&+ I_{6F2}M_2 + \hat{L}_{6D3}M_2 + \hat{L}_{4s}M_{4a} - 3\hat{L}_{4s}\hat{L}_2 M_2 - \hat{L}_{4c(1')}\hat{B}_2 M_2 \\
&- \hat{L}_{4c(2')}\hat{B}_2 M_2 - M_{4a(2^*)}\delta m_2 \hat{L}_2 - M_{4a}\hat{B}_2 \hat{L}_2 - M_{4a}\hat{B}_2 \hat{L}_{2'} + 3\hat{B}_2 \hat{L}_2 M_2 \hat{L}_{2'}
\end{aligned}$$

$$\begin{aligned}
M_{10} = & \Delta M_{10} + M_{6B}\hat{L}_2 + M_{6D}\hat{B}_2 + M_{6D(2^*)}\delta m_2 + \hat{L}_{6B1}M_2 \\
& + I_{6D2}M_2 + \delta\hat{m}_{4b}M_{4a(1^*)} - \delta\hat{m}_{4b}\hat{L}_2M_{2^*} + \hat{B}_{4b}M_{4a} - \hat{B}_{4b}\hat{L}_2M_2 \\
& - \hat{B}_{4b}M_2\hat{L}_{2'} + \Delta\delta m_{4b}I_{4a(1^*)} - \hat{L}_{4s(2')} \hat{B}_2M_2 - M_{4a(1^*)}\delta m_2\delta\hat{m}_{2^*} - M_{4a(1^*)}\hat{B}_2\delta\hat{m}_{2'} \\
& - M_{4b(2^*)}\delta m_2\hat{L}_2 - M_{4b}\hat{B}_2\hat{L}_2 - M_{4a}\hat{B}_2\hat{B}_{2'} + \Delta M_{4b}I_{4c} + I_{4c}M_2I_2 \\
& + \delta m_2\hat{L}_2\delta\hat{m}_{2^*}M_{2^*} + \hat{B}_2\hat{L}_2M_{2^*}\delta\hat{m}_{2'} + \hat{B}_2\hat{L}_2M_2\hat{B}_{2'} + \hat{B}_2M_2\hat{B}_{2'}\hat{L}_{2'}
\end{aligned}$$

$$\begin{aligned}
M_{11} = & \Delta M_{11} + 2M_{6D}\hat{B}_2 + 2M_{6D(5^*)}\delta m_2 + 2I_{6D5}M_2 + 2\hat{L}_{4s}M_{4b} \\
& - 2\hat{L}_{4s}\delta m_2M_{2^*} - 2\hat{L}_{4s}\hat{B}_2M_2 + 2\Delta L_{4s}M_2I_2 - 2M_{4a(1^*)}\delta m_2\hat{B}_2 - 2M_{4b}\hat{B}_2\hat{L}_{2'} \\
& - M_{4a}(\hat{B}_2)^2 - M_{4a(1^*3^*)}(\delta m_2)^2 + 2\delta m_2\hat{B}_2M_{2^*}\hat{L}_{2'} + 2(\hat{B}_2)^2M_2\hat{L}_{2'}
\end{aligned}$$

$$\begin{aligned}
M_{12} = & \Delta M_{12} + 3M_{6A}\hat{B}_2 + 2M_{6A(1^*)}\delta m_2 + M_{6A(3^*)}\delta m_2 + 2I_{6A1}M_2 \\
& + I_{6A3}M_2 - 6M_{4b(1^*)}\delta m_2\hat{B}_2 - 3M_{4b}(\hat{B}_2)^2 - 2M_{4b(1^*1^*)}(\delta m_2)^2 - M_{4b(1^*3^*)}(\delta m_2)^2 \\
& + 3\delta m_2(\hat{B}_2)^2M_{2^*} + 3(\delta m_2)^2\hat{B}_2M_{2^{**}} + (\delta m_2)^3M_{2^{***}} + (\hat{B}_2)^3M_2
\end{aligned}$$

$$\begin{aligned}
M_{13} = & \Delta M_{13} + M_{6H}\hat{B}_2 + M_{6H(1^*)}\delta m_2 + I_{6H1}M_2 + \hat{L}_{6D4}M_2 \\
& + \hat{L}_{4x}M_{4b} - \hat{L}_{4x}\delta m_2M_{2^*} - \hat{L}_{4x}\hat{B}_2M_2 + \Delta L_{4x}M_2I_2 - \hat{L}_{4x(1')} \hat{B}_2M_2
\end{aligned}$$

$$\begin{aligned}
M_{14} = & \Delta M_{14} + M_{6D}\hat{L}_2 + M_{6G}\hat{B}_2 + M_{6G(5^*)}\delta m_2 + \hat{L}_{6D3}M_2 \\
& + I_{6G5}M_2 - \hat{L}_{4s}\hat{L}_2M_2 + \hat{L}_{4l}M_{4b} - \hat{L}_{4l}\delta m_2M_{2^*} - \hat{L}_{4l}\hat{B}_2M_2 \\
& + \Delta L_{4l}M_2I_2 - \hat{L}_{4c(1')} \hat{B}_2M_2 - M_{4a(1^*)}\delta m_2\hat{L}_2 - M_{4b}(\hat{L}_2)^2 - M_{4a}\hat{B}_2\hat{L}_2 \\
& + \delta m_2(\hat{L}_2)^2M_{2^*} + \hat{B}_2\hat{L}_2M_2\hat{L}_{2'} + \hat{B}_2(\hat{L}_2)^2M_2
\end{aligned}$$

$$\begin{aligned}
M_{15} = & \Delta M_{15} + M_{6D}\hat{L}_2 + M_{6G}\hat{B}_2 + M_{6G(1^*)}\delta m_2 + I_{6G1}M_2 \\
& + \hat{L}_{6A2}M_2 + \hat{L}_{4c}M_{4b} - \hat{L}_{4c}\delta m_2M_{2^*} - \hat{L}_{4c}\hat{B}_2M_2 - \hat{L}_{4s}\hat{L}_2M_2 \\
& + \Delta L_{4c}M_2I_2 - \hat{L}_{4l(1')} \hat{B}_2M_2 - M_{4a(1^*)}\delta m_2\hat{L}_2 - M_{4b}(\hat{L}_2)^2 - M_{4a}\hat{B}_2\hat{L}_2 \\
& + \delta m_2(\hat{L}_2)^2M_{2^*} + \hat{B}_2\hat{L}_2M_2\hat{L}_{2'} + \hat{B}_2(\hat{L}_2)^2M_2
\end{aligned}$$

$$\begin{aligned}
M_{16} = & \Delta M_{16} + 2M_{6A}\hat{L}_2 + M_{6C}\hat{B}_2 + M_{6C(1^*)}\delta m_2 + I_{6C1}M_2 \\
& + 1/2J_{6C}M_2 + \delta\hat{m}_{4a}M_{4b(1^*)} - \delta\hat{m}_{4a}\delta m_2M_{2^{**}} - \delta\hat{m}_{4a}\hat{B}_2M_{2^*} + \hat{B}_{4a}M_{4b} \\
& - \hat{B}_{4a}\delta m_2M_{2^*} - \hat{B}_{4a}\hat{B}_2M_2 + \Delta\delta m_{4a}I_{4b(1^*)} - \Delta\delta m_{4a}M_2I_{2^*} - 4M_{4b(1^*)}\delta m_2\hat{L}_2 \\
& - 4M_{4b}\hat{B}_2\hat{L}_2 + \Delta M_{4a}I_{4s} + 4\delta m_2\hat{B}_2\hat{L}_2M_{2^*} + 2(\delta m_2)^2\hat{L}_2M_{2^{**}} + 2(\hat{B}_2)^2\hat{L}_2M_2
\end{aligned}$$

$$\begin{aligned}
M_{17} = & \Delta M_{17} + M_{6D}\hat{B}_2 + M_{6E}\hat{B}_2 + M_{6E(1*)}\delta m_2 + M_{6D(4*)}\delta m_2 \\
& + I_{6E1}M_2 + \hat{L}_{6A3}M_2 + I_{6D4}M_2 + \hat{L}_{4s}M_{4b} - \hat{L}_{4s}\delta m_2 M_{2*} \\
& - \hat{L}_{4s}\hat{B}_2 M_2 + \Delta L_{4s}M_2 I_2 - 2\hat{L}_{4s(1')}\hat{B}_2 M_2 - M_{4a(1*)}\delta m_2 \hat{B}_2 - M_{4a(2*)}\delta m_2 \hat{B}_2 \\
& - M_{4b}\hat{B}_2 \hat{L}_{2'} - M_{4a}(\hat{B}_2)^2 - M_{4a(1*2*)}(\delta m_2)^2 + \hat{L}_{2''}(\hat{B}_2)^2 M_2 + \delta m_2 \hat{B}_2 M_{2*} \hat{L}_{2'} \\
& + (\hat{B}_2)^2 M_2 \hat{L}_{2'}
\end{aligned}$$

$$\begin{aligned}
M_{18} = & \Delta M_{18} + M_{6A}\hat{B}_2 + M_{6B}\hat{B}_2 + M_{6B(1*)}\delta m_2 + M_{6A(2*)}\delta m_2 \\
& + I_{6B1}M_2 + I_{6A2}M_2 + 1/2 J_{6B}M_2 + \delta \hat{m}_{4b}M_{4b(1*)} - \delta \hat{m}_{4b}\delta m_2 M_{2**} \\
& - \delta \hat{m}_{4b}\hat{B}_2 M_{2*} + \hat{B}_{4b}M_{4b} - \hat{B}_{4b}\delta m_2 M_{2*} - \hat{B}_{4b}\hat{B}_2 M_2 + \Delta \delta m_{4b}I_{4b(1*)} \\
& - \Delta \delta m_{4b}M_2 I_{2*} - M_{4b(1*)}\delta m_2 \hat{B}_2 - M_{4b(1*)}\delta m_2 \delta \hat{m}_{2*} - M_{4b(1*)}\hat{B}_2 \delta \hat{m}_{2'} - M_{4b(2*)}\delta m_2 \hat{B}_2 \\
& - M_{4b}\hat{B}_2 \hat{B}_{2'} - M_{4b}(\hat{B}_2)^2 - M_{4b(1*2*)}(\delta m_2)^2 + \Delta M_{4b}I_{4s} + I_{4s}M_2 I_2 \\
& + \delta m_2 \hat{B}_2 \delta \hat{m}_{2*} M_{2*} + \delta m_2 \hat{B}_2 M_{2*} \hat{B}_{2'} + \delta m_2 \hat{B}_2 M_{2**} \delta \hat{m}_{2'} + (\delta m_2)^2 \delta \hat{m}_{2*} M_{2**} + (\hat{B}_2)^2 M_{2*} \delta \hat{m}_{2'} \\
& + (\hat{B}_2)^2 M_2 \hat{B}_{2'}
\end{aligned}$$

$$M_{19} = \Delta M_{19} + 2\hat{L}_{6H2}M_2$$

$$M_{20} = \Delta M_{20} + M_{6H}\hat{L}_2 + \hat{L}_{6F2}M_2 + \hat{L}_{6G4}M_2 - 2\hat{L}_{4x}\hat{L}_2 M_2$$

$$M_{21} = \Delta M_{21} + 2\hat{L}_{6G2}M_2$$

$$\begin{aligned}
M_{22} = & \Delta M_{22} + M_{6G}\hat{L}_2 + \hat{L}_{6F1}M_2 + \hat{L}_{6C2}M_2 + \hat{L}_{4c}M_{4a} \\
& - 3\hat{L}_{4c}\hat{L}_2 M_2 - \hat{L}_{4l}\hat{L}_2 M_2 - M_{4a}(\hat{L}_2)^2 + 2(\hat{L}_2)^3 M_2
\end{aligned}$$

$$\begin{aligned}
M_{23} = & \Delta M_{23} + M_{6H}\hat{B}_2 + M_{6H(2*)}\delta m_2 + \hat{L}_{6E2}M_2 + I_{6H2}M_2 \\
& + \hat{L}_{6D4}M_2 - \hat{L}_{4x(1')}\hat{B}_2 M_2 - \hat{L}_{4x(2')}\hat{B}_2 M_2
\end{aligned}$$

$$\begin{aligned}
M_{24} = & \Delta M_{24} + M_{6G}\hat{B}_2 + M_{6G(2*)}\delta m_2 + \hat{L}_{6B2}M_2 + I_{6G2}M_2 \\
& + \hat{L}_{6D5}M_2 + \hat{L}_{4s}M_{4a} - 2\hat{L}_{4s}\hat{L}_2 M_2 - \hat{L}_{4c(3')}\hat{B}_2 M_2 - \hat{L}_{4l(2')}\hat{B}_2 M_2 \\
& - M_{4a}\hat{B}_2 \hat{L}_{2'} + 2\hat{B}_2 \hat{L}_2 M_2 \hat{L}_{2'}
\end{aligned}$$

$$M_{25} = \Delta M_{25} + 2M_{6G}\hat{L}_2 + 2\hat{L}_{6D2}M_2 - 2\hat{L}_{4c}\hat{L}_2M_2 - 2\hat{L}_{4l}\hat{L}_2M_2 \\ - M_{4a}(\hat{L}_2)^2 + 2(\hat{L}_2)^3M_2$$

$$M_{26} = \Delta M_{26} + \Delta M_{6F}I_2 + 2M_{6C}\hat{L}_2 + \delta\hat{m}_{6F}M_{2^*} + \hat{B}_{6F}M_2 \\ + \Delta\delta m_{6F}M_{2^*}[I] - 2\delta\hat{m}_{4a}\hat{L}_2M_{2^*} - 2\hat{B}_{4a}\hat{L}_2M_2 + 2\hat{L}_{4c}M_{4b} - 2\hat{L}_{4c}\delta m_2M_{2^*} \\ - 2\hat{L}_{4c}\hat{B}_2M_2 - 3M_{4b}(\hat{L}_2)^2 + 3\delta m_2(\hat{L}_2)^2M_{2^*} + 3\hat{B}_2(\hat{L}_2)^2M_2$$

$$M_{27} = \Delta M_{27} + M_{6E}\hat{L}_2 + M_{6G}\hat{B}_2 + M_{6G(4^*)}\delta m_2 + \hat{L}_{6D1}M_2 \\ + \hat{L}_{6A2}M_2 + I_{6G4}M_2 - 2\hat{L}_{4s}\hat{L}_2M_2 - \hat{L}_{4c((1')')} \hat{B}_2M_2 - \hat{L}_{4l(1')} \hat{B}_2M_2 \\ - M_{4a(2^*)}\delta m_2\hat{L}_2 - M_{4a}\hat{B}_2\hat{L}_2 + 2\hat{B}_2\hat{L}_2M_2\hat{L}_2'$$

$$M_{28} = \Delta M_{28} + \Delta M_{6D}I_2 + M_{6B}\hat{L}_2 + M_{6C}\hat{B}_2 + M_{6C(2^*)}\delta m_2 \\ + \delta\hat{m}_{6D}M_{2^*} + I_{6C2}M_2 + \hat{B}_{6D}M_2 + \Delta\delta m_{6D}M_{2^*}[I] - \delta\hat{m}_{4b}\hat{L}_2M_{2^*} \\ - \hat{B}_{4b}\hat{L}_2M_2 + \hat{L}_{4s}M_{4b} - \hat{L}_{4s}\delta m_2M_{2^*} - \hat{L}_{4s}\hat{B}_2M_2 - \delta\hat{m}_{4a(1^*)}\delta m_2M_{2^*} \\ - \delta\hat{m}_{4a(1')}\hat{B}_2M_{2^*} - \hat{B}_{4a(1')}\hat{B}_2M_2 - M_{4b(2^*)}\delta m_2\hat{L}_2 - M_{4b}\hat{B}_2\hat{L}_2 - M_{4b}\hat{B}_2\hat{L}_2' \\ + I_{4c}M_2I_2 + \delta m_2\hat{B}_2M_{2^*}\hat{L}_2' + \delta m_2\hat{L}_2\delta\hat{m}_{2^*}M_{2^*} + \hat{B}_2\hat{L}_2M_{2^*}\delta\hat{m}_{2'} + \hat{B}_2\hat{L}_2M_2\hat{B}_2' \\ + (\hat{B}_2)^2M_2\hat{L}_2'$$

$$M_{29} = \Delta M_{29} + 2M_{6E}\hat{B}_2 + 2M_{6E(2^*)}\delta m_2 + 2\hat{L}_{6A1}M_2 + 2I_{6E2}M_2 \\ - 2\hat{L}_{4s((1')')} \hat{B}_2M_2 - 2\hat{L}_{4s(3')} \hat{B}_2M_2 - 2M_{4a(2^*)}\delta m_2\hat{B}_2 - M_{4a}(\hat{B}_2)^2 - M_{4a(2^*2^*)}(\delta m_2)^2 \\ + 2\hat{L}_{2''}(\hat{B}_2)^2M_2$$

$$M_{30} = \Delta M_{30} + \Delta M_{6A}I_2 + 2M_{6B}\hat{B}_2 + 2M_{6B(2^*)}\delta m_2 + \delta\hat{m}_{6A}M_{2^*} \\ + 2I_{6B2}M_2 + \hat{B}_{6A}M_2 + \Delta\delta m_{6A}M_{2^*}[I] - 2\delta\hat{m}_{4b(1^*)}\delta m_2M_{2^*} - 2\delta\hat{m}_{4b(1')}\hat{B}_2M_{2^*} \\ - 2\hat{B}_{4b(1')}\hat{B}_2M_2 - 2M_{4b(2^*)}\delta m_2\hat{B}_2 - M_{4b}(\hat{B}_2)^2 - M_{4b(2^*2^*)}(\delta m_2)^2 + 2I_{4s}M_2I_2 \\ + 2\delta m_2\hat{B}_2\delta\hat{m}_{2^*}M_{2^*} + (\hat{B}_2)^2M_{2^*}\delta\hat{m}_{2''} + (\hat{B}_2)^2M_2\hat{B}_2''$$

$$M_{31} = \Delta M_{31} + 2\hat{L}_{6H3}M_2$$

$$M_{32} = \Delta M_{32} + \hat{L}_{6H2}M_2 + \hat{L}_{6G3}M_2$$

$$M_{33} = \Delta M_{33} + 2\hat{L}_{6G3}M_2$$

$$M_{34} = \Delta M_{34} + \hat{L}_{6H1}M_2 + \hat{L}_{6C3}M_2 + \hat{L}_{4x}M_{4a} - 2\hat{L}_{4x}\hat{L}_2M_2$$

$$M_{35} = \Delta M_{35} + M_{6H}\hat{L}_2 + \hat{L}_{6E3}M_2 + \hat{L}_{6G4}M_2 - 2\hat{L}_{4x}\hat{L}_2M_2$$

$$M_{36} = \Delta M_{36} + M_{6G}\hat{L}_2 + \hat{L}_{6B3}M_2 + \hat{L}_{6G5}M_2 - \hat{L}_{4c}\hat{L}_2M_2 \\ + \hat{L}_{4l}M_{4a} - 3\hat{L}_{4l}\hat{L}_2M_2 - M_{4a}(\hat{L}_2)^2 + 2(\hat{L}_2)^3M_2$$

$$M_{37} = \Delta M_{37} + 2\hat{L}_{6G2}M_2$$

$$M_{38} = \Delta M_{38} + \Delta M_{6H}I_2 + \delta\hat{m}_{6H}M_{2^*} + \hat{B}_{6H}M_2 + \Delta\delta m_{6H}M_{2^*}[I] \\ + 2\hat{L}_{4x}M_{4b} - 2\hat{L}_{4x}\delta m_2M_{2^*} - 2\hat{L}_{4x}\hat{B}_2M_2$$

$$M_{39} = \Delta M_{39} + M_{6G}\hat{L}_2 + \hat{L}_{6G1}M_2 + \hat{L}_{6C2}M_2 + \hat{L}_{4c}M_{4a} \\ - 3\hat{L}_{4c}\hat{L}_2M_2 - \hat{L}_{4l}\hat{L}_2M_2 - M_{4a}(\hat{L}_2)^2 + 2(\hat{L}_2)^3M_2$$

$$M_{40} = \Delta M_{40} + \Delta M_{6G}I_2 + M_{6C}\hat{L}_2 + \delta\hat{m}_{6G}M_{2^*} + \hat{B}_{6G}M_2 \\ + \Delta\delta m_{6G}M_{2^*}[I] - \delta\hat{m}_{4a}\hat{L}_2M_{2^*} - \hat{B}_{4a}\hat{L}_2M_2 + \hat{L}_{4c}M_{4b} - \hat{L}_{4c}\delta m_2M_{2^*} \\ - \hat{L}_{4c}\hat{B}_2M_2 + \hat{L}_{4l}M_{4b} - \hat{L}_{4l}\delta m_2M_{2^*} - \hat{L}_{4l}\hat{B}_2M_2 - 2M_{4b}(\hat{L}_2)^2 \\ + 2\delta m_2(\hat{L}_2)^2M_{2^*} + 2\hat{B}_2(\hat{L}_2)^2M_2$$

$$M_{41} = \Delta M_{41} + 2M_{6E}\hat{L}_2 + 2\hat{L}_{6C1}M_2 + \delta\hat{m}_{4a}M_{4a(2^*)} + \hat{B}_{4a}M_{4a} \\ - 2\hat{B}_{4a}M_2\hat{L}_{2'} - 4\hat{L}_{4s}\hat{L}_2M_2 + \Delta\delta m_{4a}I_{4a(2^*)} - 2M_{4a(2^*)}\delta m_2\hat{L}_2 - 2M_{4a}\hat{B}_2\hat{L}_2 \\ + \Delta M_{4a}I_{4x} + 4\hat{B}_2\hat{L}_2M_2\hat{L}_{2'}$$

$$M_{42} = \Delta M_{42} + \Delta M_{6C}I_2 + 2M_{6B}\hat{L}_2 + \delta\hat{m}_{6C}M_{2^*} + \hat{B}_{6C}M_2 \\ + \Delta\delta m_{6C}M_{2^*}[I] + \delta\hat{m}_{4a}M_{4b(2^*)} - \delta\hat{m}_{4a}\delta\hat{m}_{2^*}M_{2^*} - 2\delta\hat{m}_{4b}\hat{L}_2M_{2^*} + \hat{B}_{4a}M_{4b} \\ - \hat{B}_{4a}M_{2^*}\delta\hat{m}_{2'} - \hat{B}_{4a}M_2\hat{B}_{2'} - 2\hat{B}_{4b}\hat{L}_2M_2 + \Delta\delta m_{4a}I_{4b(2^*)} - 2M_{4b(2^*)}\delta m_2\hat{L}_2 \\ - 2M_{4b}\hat{B}_2\hat{L}_2 + \Delta M_{4a}I_{4l} + \Delta M_{4a}(I_2)^2 + 2\delta m_2\hat{L}_2\delta\hat{m}_{2^*}M_{2^*} + 2\hat{B}_2\hat{L}_2M_{2^*}\delta\hat{m}_{2'} \\ + 2\hat{B}_2\hat{L}_2M_2\hat{B}_{2'}$$

$$M_{43} = \Delta M_{43} + M_{6H}\hat{B}_2 + M_{6H(3^*)}\delta m_2 + 2\hat{L}_{6E2}M_2 + I_{6H3}M_2 \\ - 2\hat{L}_{4x(2')}\hat{B}_2M_2$$

$$M_{44} = \Delta M_{44} + M_{6G}\hat{B}_2 + M_{6G(3^*)}\delta m_2 + \hat{L}_{6E1}M_2 + \hat{L}_{6B2}M_2 \\ + I_{6G3}M_2 + \hat{L}_{4s}M_{4a} - 2\hat{L}_{4s}\hat{L}_2M_2 - \hat{L}_{4c(2')}\hat{B}_2M_2 - \hat{L}_{4l(2')}\hat{B}_2M_2 \\ - M_{4a}\hat{B}_2\hat{L}_{2'} + 2\hat{B}_2\hat{L}_2M_2\hat{L}_{2'}$$

$$M_{45} = \Delta M_{45} + \Delta M_{6E}I_2 + M_{6C}\hat{B}_2 + M_{6C(3^*)}\delta m_2 + \delta\hat{m}_{6E}M_{2^*} \\ + I_{6C3}M_2 + \hat{B}_{6E}M_2 + \Delta\delta m_{6E}M_{2^*}[I] + 2\hat{L}_{4s}M_{4b} - 2\hat{L}_{4s}\delta m_2M_{2^*} \\ - 2\hat{L}_{4s}\hat{B}_2M_2 - \delta\hat{m}_{4a(2^*)}\delta m_2M_{2^*} - \delta\hat{m}_{4a(2')}\hat{B}_2M_{2^*} - \hat{B}_{4a(2')}\hat{B}_2M_2 - 2M_{4b}\hat{B}_2\hat{L}_{2'} \\ + I_{4x}M_2I_2 + 2\delta m_2\hat{B}_2M_{2^*}\hat{L}_{2'} + 2(\hat{B}_2)^2M_2\hat{L}_{2'}$$

$$M_{46} = \Delta M_{46} + M_{6E}\hat{B}_2 + M_{6E(3^*)}\delta m_2 + 2\hat{L}_{6B1}M_2 + I_{6E3}M_2 \\ + \delta\hat{m}_{4b}M_{4a(2^*)} + \hat{B}_{4b}M_{4a} - 2\hat{B}_{4b}M_2\hat{L}_{2'} + \Delta\delta m_{4b}I_{4a(2^*)} - 2\hat{L}_{4s(2')}\hat{B}_2M_2 \\ - M_{4a(2^*)}\delta m_2\delta\hat{m}_{2^*} - M_{4a(2^*)}\hat{B}_2\delta\hat{m}_{2'} - M_{4a}\hat{B}_2\hat{B}_{2'} + \Delta M_{4b}I_{4x} + I_{4x}M_2I_2 \\ + 2\hat{B}_2M_2\hat{B}_{2'}\hat{L}_{2'}$$

$$M_{47} = \Delta M_{47} + \Delta M_{6B}I_2 + M_{6B}\hat{B}_2 + M_{6B(3^*)}\delta m_2 + \delta\hat{m}_{6B}M_{2^*} \\ + I_{6B3}M_2 + \hat{B}_{6B}M_2 + \Delta\delta m_{6B}M_{2^*}[I] + \delta\hat{m}_{4b}M_{4b(2^*)} - \delta\hat{m}_{4b}\delta\hat{m}_{2^*}M_{2^*} \\ + \hat{B}_{4b}M_{4b} - \hat{B}_{4b}M_{2^*}\delta\hat{m}_{2'} - \hat{B}_{4b}M_2\hat{B}_{2'} - \delta\hat{m}_{4b(2^*)}\delta m_2M_{2^*} - \delta\hat{m}_{4b(2')}\hat{B}_2M_{2^*} \\ - \hat{B}_{4b(2')}\hat{B}_2M_2 + \Delta\delta m_{4b}I_{4b(2^*)} - M_{4b(2^*)}\delta m_2\delta\hat{m}_{2^*} - M_{4b(2^*)}\hat{B}_2\delta\hat{m}_{2'} - M_{4b}\hat{B}_2\hat{B}_{2'} \\ + \Delta M_{4b}I_{4l} + \Delta M_{4b}(I_2)^2 + 2I_{4l}M_2I_2 + \delta m_2(\delta\hat{m}_{2^*})^2M_{2^*} + \hat{B}_2\delta\hat{m}_{2^*}M_{2^*}\delta\hat{m}_{2'} \\ + \hat{B}_2M_{2^*}\delta\hat{m}_{2'}\hat{B}_{2'} + \hat{B}_2M_2(\hat{B}_{2'})^2 + M_2(I_2)^3$$

2. Divergence Structure of Quantities of Sixth- and Lower-Orders

Substitution of M_i into a_i expresses the latter in terms of finite quantity ΔM_i . However, a_i still contains numerous (divergent) quantities of lower orders. To obtain a finite result in the end we need the information on the divergence structure of these quantities, which

are listed in the following. The suffix 6α , ($\alpha = A, \dots, H$), in $L_{6\alpha}$, $B_{6\alpha}$, $\delta m_{6\alpha}$ refers to the diagrams similar to those of Fig. 5, before Π_2 insertion is made.

Vertex renormalization constants of sixth-order

$$L_{6A1} = I_{6A1} + \Delta L_{6A1} + 2\delta m_2 L_{4s(1^*)} + 2\hat{B}_2 \tilde{L}_{4s(1')} - \delta m_2 (\delta m_2 L_{2^{**\dagger}} + \hat{B}_2 L_{2'^*}) - \hat{B}_2 (\delta m_2 L_{2'^*} + \hat{B}_2 \tilde{L}_{2''}) + \hat{L}_{6A1}$$

$$L_{6A2} = I_{6A2} + \Delta L_{6A2} + \hat{L}_2 \tilde{L}_{4s} + \delta m_2 L_{4l(1^*)} + \hat{B}_2 \tilde{L}_{4l(1')} - \hat{L}_2 (\delta m_2 L_{2^*} + \hat{B}_2 \tilde{L}_{2'}) + I_{4s} \tilde{L}_2 + \hat{L}_{6A2}$$

$$L_{6A3} = I_{6A3} + \Delta L_{6A3} + 2(\delta m_2 L_{4s(1^*)} + \hat{B}_2 \tilde{L}_{4s(1')}) - \delta m_2 (\delta m_2 L_{2^{*\dagger}} + \hat{B}_2 L_{2'^*}) - \hat{B}_2 (\delta m_2 L_{2'^*} + \hat{B}_2 \tilde{L}_{2''}) + \hat{L}_{6A3}$$

$$L_{6B1} = I_{6B1} + \Delta L_{6B1} + \delta m_2 L_{4s(2^*)} + \hat{B}_2 \tilde{L}_{4s(2')} + \delta \hat{m}_{4b} L_{2^*} + \hat{B}_{4b} \tilde{L}_{2'} - \delta m_2 \delta \hat{m}_{2^*} L_{2^*} - \hat{B}_2 (\delta \hat{m}_{2'} L_{2^*} + \hat{B}_{2'} \tilde{L}_{2'}) + 1/2 J_{6B} + \hat{L}_{6B1}$$

$$L_{6B2} = I_{6B2} + \Delta L_{6B2} + \delta m_2 L_{4l(2^*)} + \hat{B}_2 \tilde{L}_{4l(2')} + \hat{L}_{4s} \tilde{L}_2 - \hat{B}_2 \hat{L}_{2'} \tilde{L}_2 + I_2 \tilde{L}_{4s} - I_2 (\delta m_2 L_{2^*} + \hat{B}_2 \tilde{L}_{2'}) + \hat{L}_{6B2}$$

$$L_{6B3} = I_{6B3} + \Delta L_{6B3} + \hat{L}_2 \tilde{L}_{4l} + \hat{L}_{4l} \tilde{L}_2 - (\hat{L}_2)^2 \tilde{L}_2 + I_2 \tilde{L}_{4l} - I_2 \hat{L}_2 \tilde{L}_2 + I_{4l} \tilde{L}_2 + \hat{L}_{6B3}$$

$$L_{6C1} = I_{6C1} + \Delta L_{6C1} + 2\hat{L}_2 \tilde{L}_{4s} + \delta \hat{m}_{4a} L_{2^*} + \hat{B}_{4a} \tilde{L}_{2'} - 2\hat{L}_2 (\delta m_2 L_{2^*} + \hat{B}_2 \tilde{L}_{2'}) + 1/2 J_{6C} + \hat{L}_{6C1}$$

$$L_{6C2} = I_{6C2} + \Delta L_{6C2} + \hat{L}_2 \tilde{L}_{4l} + \hat{L}_{4c} \tilde{L}_2 - (\hat{L}_2)^2 \tilde{L}_2 + I_2 \tilde{L}_{4c} - I_2 \hat{L}_2 \tilde{L}_2 + \hat{L}_{6C2}$$

$$L_{6C3} = I_{6C3} + \Delta L_{6C3} + \hat{L}_{4x} \tilde{L}_2 + I_2 \tilde{L}_{4x} + \hat{L}_{6C3}$$

$$L_{6D1} = I_{6D1} + \Delta L_{6D1} + \delta m_2 L_{4c(1^*)} + \hat{B}_2 \tilde{L}_{4c(1')} + \hat{L}_2 \tilde{L}_{4s} \\ - \hat{L}_2 (\delta m_2 L_{2^*} + \hat{B}_2 \tilde{L}_{2'}) + \hat{L}_{6D1}$$

$$L_{6D2} = I_{6D2} + \Delta L_{6D2} + \hat{L}_2 \tilde{L}_{4c} + \hat{L}_2 \tilde{L}_{4l} - (\hat{L}_2)^2 \tilde{L}_2 + I_{4c} \tilde{L}_2 + \hat{L}_{6D2}$$

$$L_{6D3} = I_{6D3} + \Delta L_{6D3} + \delta m_2 L_{4c(1^*)} + \hat{B}_2 \tilde{L}_{4c(1')} + \hat{L}_2 \tilde{L}_{4s} \\ - \hat{L}_2 (\delta m_2 L_{2^*} + \hat{B}_2 \tilde{L}_{2'}) + \hat{L}_{6D3}$$

$$L_{6D4} = I_{6D4} + \Delta L_{6D4} + \delta m_2 L_{4x(1^*)} + \hat{B}_2 \tilde{L}_{4x(1')} + \hat{L}_{6D4}$$

$$L_{6D5} = I_{6D5} + \Delta L_{6D5} + \delta m_2 L_{4c(3^*)} + \hat{B}_2 \tilde{L}_{4c(3')} + \hat{L}_{4s} \tilde{L}_2 \\ - \hat{B}_2 \hat{L}_{2'} \tilde{L}_2 + I_2 \Delta L_{4s} + \hat{L}_{6D5}$$

$$L_{6E1} = I_{6E1} + \Delta L_{6E1} + \delta m_2 L_{4c(2^*)} + \hat{B}_2 \tilde{L}_{4c(2')} + \hat{L}_{4s} \tilde{L}_2 \\ - \hat{B}_2 \hat{L}_{2'} \tilde{L}_2 + I_2 \Delta L_{4s} + \hat{L}_{6E1}$$

$$L_{6E2} = I_{6E2} + \Delta L_{6E2} + \delta m_2 L_{4x(2^*)} + \hat{B}_2 \tilde{L}_{4x(2')} + \hat{L}_{6E2}$$

$$L_{6E3} = I_{6E3} + \Delta L_{6E3} + I_{4x} \tilde{L}_2 + \hat{L}_2 \tilde{L}_{4x} + \hat{L}_{6E3}$$

$$L_{6F1} = I_{6F1} + \Delta L_{6F1} + \hat{L}_2 \tilde{L}_{4c} + \hat{L}_{4c} \tilde{L}_2 - (\hat{L}_2)^2 \tilde{L}_2 + I_2 \Delta L_{4c} + \hat{L}_{6F1}$$

$$L_{6F2} = I_{6F2} + \Delta L_{6F2} + \hat{L}_2 \tilde{L}_{4x} + \hat{L}_{6F2}$$

$$L_{6F3} = I_{6F3} + \Delta L_{6F3} + 2\hat{L}_2 \tilde{L}_{4c} - (\hat{L}_2)^2 \tilde{L}_2 + \hat{L}_{6F3}$$

$$L_{6G1} = I_{6G1} + \Delta L_{6G1} + \hat{L}_2 \tilde{L}_{4c} + \hat{L}_{4c} \tilde{L}_2 - (\hat{L}_2)^2 \tilde{L}_2 + I_2 \Delta L_{4c} + \hat{L}_{6G1}$$

$$L_{6G2} = I_{6G2} + \Delta L_{6G2} + \hat{L}_{6G2}$$

$$L_{6G3} = I_{6G3} + \Delta L_{6G3} + \hat{L}_{6G3}$$

$$L_{6G4} = I_{6G4} + \Delta L_{6G4} + \hat{L}_2 \tilde{L}_{4x} + \hat{L}_{6G4}$$

$$L_{6G5} = I_{6G5} + \Delta L_{6G5} + \hat{L}_2 \tilde{L}_{4c} + \hat{L}_{4l} \tilde{L}_2 - (\hat{L}_2)^2 \tilde{L}_2 + I_2 \Delta L_{4l} + \hat{L}_{6G5}$$

$$L_{6H1} = I_{6H1} + \Delta L_{6H1} + \hat{L}_{4x} \tilde{L}_2 + I_2 \Delta L_{4x} + \hat{L}_{6H1}$$

$$L_{6H2} = I_{6H2} + \Delta L_{6H2} + \hat{L}_{6H2}$$

$$L_{6H3} = I_{6H3} + \Delta L_{6H3} + \hat{L}_{6H3}$$

Wave-function renormalization constants of sixth-order

$$\begin{aligned} B_{6A} = & - \sum_{\alpha=1}^5 I_{6A\alpha} + \Delta B_{6A} + 2(\delta m_2 B_{4b(1^*)} + \hat{B}_2 \tilde{B}_{4b(1')}) \\ & - \delta m_2 (\delta m_2 B_{2^{**}} + \hat{B}_2 B_{2^*}) - \hat{B}_2 (\delta m_2 B_{2^*} + \hat{B}_2 \tilde{B}_{2''}) + 2I_{4s} \tilde{B}_2 + \hat{B}_{6A} \end{aligned}$$

$$\begin{aligned} B_{6B} = & - \sum_{\alpha=1}^5 I_{6B\alpha} + \Delta B_{6B} + \delta m_2 B_{4b(2^*)} + \hat{B}_2 \tilde{B}_{4b(2')} \\ & + \delta \hat{m}_{4b} B_{2^*} + \hat{B}_{4b} \tilde{B}_{2'} - \delta m_2 \delta \hat{m}_{2^*} B_{2^*} - \hat{B}_2 (\delta \hat{m}_{2'} B_{2^*} + \hat{B}_{2'} \tilde{B}_{2'}) \\ & + I_2 \tilde{B}_{4b} - I_2 (\delta m_2 B_{2^*} + \hat{B}_2 \tilde{B}_{2'}) + I_{4l} \tilde{B}_2 + B_{2^*} [I] \Delta \delta m_{4b} - J_{6B} + \hat{B}_{6B} \end{aligned}$$

$$\begin{aligned} B_{6C} = & - \sum_{\alpha=1}^5 I_{6C\alpha} + \Delta B_{6C} + 2\hat{L}_2 \tilde{B}_{4b} + \delta \hat{m}_{4a} B_{2^*} + \hat{B}_{4a} \tilde{B}_{2'} \\ & - 2\hat{L}_2 (\delta m_2 B_{2^*} + \hat{B}_2 \tilde{B}_{2'}) + I_2 \tilde{B}_{4a} - 2I_2 \hat{L}_2 \tilde{B}_2 + B_{2^*} [I] \Delta \delta m_{4a} - J_{6C} + \hat{B}_{6C} \end{aligned}$$

$$\begin{aligned} B_{6D} = & - \sum_{\alpha=1}^5 I_{6D\alpha} + \Delta B_{6D} + \delta m_2 B_{4a(1^*)} + \hat{B}_2 \tilde{B}_{4a(1')} + \hat{L}_2 \tilde{B}_{4b} + \hat{L}_{4s} \tilde{B}_2 \\ & - \hat{L}_2 (\delta m_2 B_{2^*} + \hat{B}_2 \tilde{B}_{2'}) - \hat{B}_2 \hat{L}_{2'} \tilde{B}_2 + I_{4c} \tilde{B}_2 + \tilde{B}_2 \Delta L_{4s} + \hat{B}_{6D} \end{aligned}$$

$$\begin{aligned}
B_{6E} &= - \sum_{\alpha=1}^5 I_{6E\alpha} + \Delta B_{6E} + \delta m_2 B_{4a(2^*)} + \hat{B}_2 \tilde{B}_{4a(2')} \\
&\quad + 2\hat{L}_{4s} \tilde{B}_2 - 2\hat{B}_2 \hat{L}_{2'} \tilde{B}_2 + I_{4x} \tilde{B}_2 + 2\tilde{B}_2 \Delta L_{4s} + \hat{B}_{6E} \\
B_{6F} &= - \sum_{\alpha=1}^5 I_{6F\alpha} + \Delta B_{6F} + 2\hat{L}_2 \tilde{B}_{4a} + 2\hat{L}_{4c} \tilde{B}_2 - 3(\hat{L}_2)^2 \tilde{B}_2 + 2\tilde{B}_2 \Delta L_{4c} + \hat{B}_{6F} \\
B_{6G} &= - \sum_{\alpha=1}^5 I_{6G\alpha} + \Delta B_{6G} + \hat{L}_2 \tilde{B}_{4a} + \hat{L}_{4c} \tilde{B}_2 \\
&\quad + \hat{L}_{4l} \tilde{B}_2 - 2(\hat{L}_2)^2 \tilde{B}_2 + \tilde{B}_2 (\Delta L_{4l} + \Delta L_{4c}) + \hat{B}_{6G} \\
B_{6H} &= - \sum_{\alpha=1}^5 I_{6H\alpha} + \Delta B_{6H} + 2\hat{L}_{4x} \tilde{B}_2 + 2\tilde{B}_2 \Delta L_{4x} + \hat{B}_{6H}
\end{aligned}$$

Mass renormalization constants of sixth-order

$$\begin{aligned}
\delta m_{6A} &= \Delta \delta m_{6A} + 2(\delta m_2 \delta \tilde{m}_{4b(1^*)} + \hat{B}_2 \delta \tilde{m}_{4b(1')}) - \delta m_2 (\delta m_2 \delta m_{2^{**}} + \hat{B}_2 \delta \tilde{m}_{2'^*}) \\
&\quad - \hat{B}_2 (\delta m_2 \delta \tilde{m}_{2'^*} + \hat{B}_2 \delta \tilde{m}_{2''}) + \delta \hat{m}_{6A}
\end{aligned}$$

$$\begin{aligned}
\delta m_{6B} &= \Delta \delta m_{6B} + \delta m_2 \delta \tilde{m}_{4b(2^*)} + \hat{B}_2 \delta \tilde{m}_{4b(2')} + \delta \hat{m}_{4b} \delta \tilde{m}_{2^*} + \hat{B}_{4b} \delta \tilde{m}_{2'} \\
&\quad - \delta m_2 \delta \hat{m}_{2^*} \delta \tilde{m}_{2^*} - \hat{B}_2 (\delta \hat{m}_{2'} \delta \tilde{m}_{2^*} + \hat{B}_{2'} \delta \tilde{m}_{2'}) + I_2 \delta \tilde{m}_{4b} - I_2 (\delta m_2 \delta \tilde{m}_{2^*} \\
&\quad + \hat{B}_2 \delta \tilde{m}_{2'}) + \delta \hat{m}_{6B}
\end{aligned}$$

$$\begin{aligned}
\delta m_{6C} &= \Delta \delta m_{6C} + 2\hat{L}_2 \delta \tilde{m}_{4b} + \delta \hat{m}_{4a} \delta \tilde{m}_{2^*} + \hat{B}_{4a} \delta \tilde{m}_{2'} - 2\hat{L}_2 (\delta m_2 \delta \tilde{m}_{2^*} \\
&\quad + \hat{B}_2 \delta \tilde{m}_{2'}) + I_2 \delta \tilde{m}_{4a} + \delta \hat{m}_{6C}
\end{aligned}$$

$$\begin{aligned}
\delta m_{6D} &= \Delta \delta m_{6D} + \delta m_2 \delta \tilde{m}_{4a(1^*)} + \hat{B}_2 \delta \tilde{m}_{4a(1')} + \hat{L}_2 \delta \tilde{m}_{4b} - \hat{L}_2 (\delta m_2 \delta \tilde{m}_{2^*} \\
&\quad + \hat{B}_2 \delta \tilde{m}_{2'}) + \delta \hat{m}_{6D}
\end{aligned}$$

$$\delta m_{6E} = \Delta \delta m_{6E} + \delta m_2 \delta \tilde{m}_{4a(2^*)} + \hat{B}_2 \delta \tilde{m}_{4a(2')} + \delta \hat{m}_{6E}$$

$$\delta m_{6F} = \Delta \delta m_{6F} + 2\hat{L}_2 \delta \tilde{m}_{4a} + \delta \hat{m}_{6F}$$

$$\delta m_{6G} = \Delta \delta m_{6G} + \hat{L}_2 \delta \tilde{m}_{4a} + \delta \hat{m}_{6G}$$

$$\delta m_{6H} = \Delta \delta m_{6H} + \delta \hat{m}_{6H}$$

Renormalization Scheme for Sixth-order Moment

$$\begin{aligned} a_{6A} &= M_{6A} - 2\delta m_2 M_{4b(1^*)} - 2B_2 M_{4b} + \delta m_2 (\delta m_2 M_{2^{**}} + B_2 M_{2^*}) \\ &\quad + B_2 (\delta m_2 M_{2^*} + B_2 M_2) \end{aligned}$$

$$\begin{aligned} a_{6B} &= M_{6B} - \delta m_2 M_{4b(2^*)} - B_2 M_{4b} - \delta m_{4b} M_{2^*} - B_{4b} M_2 \\ &\quad + \delta m_2 (\delta m_{2^*} M_{2^*} + B_{2^*} M_2) + B_2 (\delta m_2 M_{2^*} + B_2 M_2) \end{aligned}$$

$$a_{6C} = M_{6C} - 2L_2 M_{4b} - \delta m_{4a} M_{2^*} - B_{4a} M_2 + 2L_2 (\delta m_2 M_{2^*} + B_2 M_2)$$

$$\begin{aligned} a_{6D} &= M_{6D} - L_{4s} M_2 - \delta m_2 M_{4a(1^*)} - B_2 M_{4a} - L_2 M_{4b} \\ &\quad + B_2 L_2 M_2 + L_2 (\delta m_2 M_{2^*} + B_2 M_2) + L_{2^*} \delta m_2 M_2 \end{aligned}$$

$$a_{6E} = M_{6E} - 2L_{4s} M_2 - \delta m_2 M_{4a(2^*)} - B_2 M_{4a} + 2L_{2^*} \delta m_2 M_2 + 2L_2 B_2 M_2$$

$$a_{6F} = M_{6F} - 2L_{4c} M_2 - 2L_2 M_{4a} + 3L_2 L_2 M_2$$

$$a_{6G} = M_{6G} - L_{4c} M_2 - L_{4l} M_2 - L_2 M_{4a} + 2L_2 L_2 M_2$$

$$a_{6H} = M_{6H} - 2L_{4x} M_2$$

$$\begin{aligned} M_{6A} &= \Delta M_{6A} + 2\delta m_2 M_{4b(1^*)} + 2\hat{B}_2 M_{4b} - \delta m_2 (\delta m_2 M_{2^{**}} + \hat{B}_2 M_{2^*}) \\ &\quad - \hat{B}_2 (\delta m_2 M_{2^*} + \hat{B}_2 M_2) + 2I_{4s} M_2 \end{aligned}$$

$$\begin{aligned} M_{6B} &= \Delta M_{6B} + \delta m_2 M_{4b(2^*)} + \hat{B}_2 M_{4b} + \delta \hat{m}_{4b} M_{2^*} + \hat{B}_{4b} M_2 \\ &\quad - \delta m_2 \delta \hat{m}_{2^*} M_{2^*} - \hat{B}_2 (\delta \hat{m}_{2'} M_{2^*} + \hat{B}_{2'} M_2) + I_2 \Delta M_{4b} + M_{2^*} [I] \Delta \delta m_{4b} \\ &\quad + \{I_{4l} + (I_2)^2\} M_2 \end{aligned}$$

$$M_{6C} = \Delta M_{6C} + 2\hat{L}_2 M_{4b} + \delta\hat{m}_{4a} M_{2^*} + \hat{B}_{4a} M_2 - 2\hat{L}_2(\delta m_2 M_{2^*} + \hat{B}_2 M_2) + I_2 M_{4a} - 2I_2 \hat{L}_2 M_2 + M_{2^*} [I] \Delta \delta m_{4a}$$

$$M_{6D} = \Delta M_{6D} + \hat{L}_{4s} M_2 + \delta m_2 M_{4a(1^*)} + \hat{B}_2 M_{4a} + \hat{L}_2 M_{4b} - \hat{B}_2 \hat{L}_{2'} M_2 - \hat{L}_2(\delta m_2 M_{2^*} + \hat{B}_2 M_2) + I_{4c} M_2$$

$$M_{6E} = \Delta M_{6E} + 2\hat{L}_{4s} M_2 + \delta m_2 M_{4a(2^*)} + \hat{B}_2 M_{4a} - 2\hat{L}_{2'} \hat{B}_2 M_2 + I_{4x} M_2$$

$$M_{6F} = \Delta M_{6F} + 2\hat{L}_{4c} M_2 + 2\hat{L}_2 M_{4a} - 3\hat{L}_2 \hat{L}_2 M_2$$

$$M_{6G} = \Delta M_{6G} + \hat{L}_{4c} M_2 + \hat{L}_{4l} M_2 + \hat{L}_2 M_{4a} - 2\hat{L}_2 \hat{L}_2 M_2$$

$$M_{6H} = \Delta M_{6H} + 2\hat{L}_{4x} M_2$$

Various Fourth-Order Quantities

$$\delta m_{4a} = \delta\hat{m}_{4a} + \Delta\delta m_{4a}$$

$$\delta m_{4b} = \delta\hat{m}_{4b} + \Delta\delta m_{4b} + \delta m_2 \delta\tilde{m}_{2^*} + \hat{B}_2 \delta\tilde{m}_{2'}$$

$$\tilde{L}_{4c((1')')} = \tilde{L}_{4c(1')}$$

$$\tilde{L}_{4s((1')')} = \tilde{L}_{4s(1')}$$

$$L_{4x} = \hat{L}_{4x} + I_{4x} + \Delta L_{4x}$$

$$\tilde{L}_{4x} = I_{4x} + \Delta L_{4x}$$

$$L_{4c} = \hat{L}_{4c} + I_{4c} + \Delta L_{4c} + \hat{L}_2 \tilde{L}_2$$

$$\tilde{L}_{4c} = I_{4c} + \Delta L_{4c} + \hat{L}_2 \tilde{L}_2$$

$$B_{4a} = \hat{B}_{4a} - I_{4x} + \Delta B_{4a} + 2\hat{L}_2\tilde{B}_2 - 2I_{4c}$$

$$\tilde{B}_{4a} = -I_{4x} + \Delta B_{4a} + 2\hat{L}_2\tilde{B}_2 - 2I_{4c}$$

$$L_{4l} = \hat{L}_{4l} + I_{4l} + (I_2)^2 + \Delta L_{4l} + \tilde{L}_2\hat{L}_2$$

$$\tilde{L}_{4l} = I_{4l} + (I_2)^2 + \Delta L_{4l} + \tilde{L}_2\hat{L}_2$$

$$L_{4s} = \hat{L}_{4s} + I_{4s} + \Delta L_{4s} + \delta m_2 L_{2^*} + \hat{B}_2\tilde{L}_{2'}$$

$$B_{4b} = \hat{B}_{4b} + \Delta B_{4b} + \delta m_2 B_{2^*} + \hat{B}_2\tilde{B}_{2'} + I_2\tilde{B}_2 - 2I_{4s} - I_{4l}$$

$$M_{4a(1^*)} = \Delta M_{4a(1^*)} + \hat{L}_2 M_{2^*} + I_{4a(1^*)}$$

$$M_{4a(2^*)} = \Delta M_{4a(2^*)} + I_{4a(2^*)}$$

$$M_{4b(1^*)} = \Delta M_{4b(1^*)} + (\delta m_2 M_{2^{**}} + \hat{B}_2 M_{2^*}) + I_{4b(1^*)}$$

$$M_{4b(2^*)} = \Delta M_{4b(2^*)} + \delta \hat{m}_{2^*} M_{2^*} + I_{4b(2^*)} + (I_2 M_{2^*} + M_{2^*} [I] \delta \tilde{m}_{2^*}) - 2M_{2^*} [I] I_2$$

$$M_{4a} = \Delta M_{4a} + 2\hat{L}_2 M_2$$

$$M_{4b} = \Delta M_{4b} + \hat{B}_2 M_2 + \delta m_2 M_{2^*} + I_2 M_2$$

$$\Delta M_{4a(2^*)} = \Delta M_{4s} - 2\Delta M_{4a(1^*)} - 2\Delta M_{4b(1^*)} - \Delta M_{4b(2^*)}$$

$$\Delta B_4 \equiv \Delta B_{4a} + \Delta B_{4b}$$

$$\Delta M_4 \equiv \Delta M_{4a} + \Delta M_{4b}$$

$$\Delta L_4 \equiv \Delta L_{4x} + 2\Delta L_{4c} + 2\Delta L_{4s} + \Delta L_{4l}$$

$$\Delta\delta m_4 \equiv \Delta\delta m_{4a} + \Delta\delta m_{4b}$$

$$2B_{4a(1^*)} + B_{4a(2^*)} = -4(3L_{4c(1^*)} + L_{4c(2^*)}) - 4(L_{4x(1^*)} + L_{4x(2^*)})$$

$$2B_{4b(1^*)} + B_{4b(2^*)} = -4(3L_{4s(1^*)} + L_{4s(2^*)}) - 4(L_{4l(1^*)} + L_{4l(2^*)})$$

Various Relations Among Second-Order Quantities

$$B_{2'} = B_2$$

$$L_{2'} = L_2$$

$$\delta\hat{m}_{2'} = \delta m_2 - \delta\tilde{m}_{2'}$$

$$\delta\hat{m}_{2''} = \delta m_2 - \delta\tilde{m}_{2''}$$

$$B_{2^{**}} = -2(2L_{2^{**}\dagger} + L_{2^{*\dagger}})$$

$$L_{2'^*} = L_{2^*} = I_{2^*} + \Delta L_{2^*}$$

$$B_{2'^*} = B_{2^*} = \Delta B_{2^*} - 2I_{2^*}$$

$$\delta\hat{m}_{2'^*} = \delta m_{2^*} - \delta\tilde{m}_{2'^*}$$

$$\delta m_{2^*} = \delta\hat{m}_{2^*} + \delta\tilde{m}_{2^*}$$

$$\delta\tilde{m}_{2^*} = I_2 + \Delta\delta m_{2^*}$$

$$B_2 = -L_2$$

$$\tilde{B}_2 = -I_2 + \Delta B_2$$

$$\hat{L}_2 = -\hat{B}_2 - \Delta B_2$$

$$\tilde{L}_2 = I_2$$

-
- [1] R. S. Van Dyck, Jr., P. B. Schwinberg, and H. G. Dehmelt, Phys. Rev. Lett. **59**, 26 (1987).
- [2] L. S. Brown and G. Gabrielse, Rev. Mod. Phys. **58**, 233 (1986); G. Gabrielse, J. Tan, and L. S. Brown, *Cavity shifts of Measure Electron Magnetic Moments*, in *Quantum Electrodynamics*, edited by T. Kinoshita (World Scientific, Singapore, 1990), pp. 389 - 418.
- [3] G. Gabrielse, Cape Cod Symposium, May 2003, <http://g2pc1.bu.edu/leptonmom>. See also G. Gabrielse and J. Tan, in *Cavity Quantum Electrodynamics*, Ed. P. Berman (Academic, New York, 1992). B. Odom, Harvard University PhD thesis, 2005.
- [4] J. Schwinger, Phys. Rev. **73**, 416L (1948).
- [5] C. M. Sommerfield, Phys. Rev. **107**, 328 (1957); Ann. Phys. (N. Y.) **5**, 26 (1958); A. Petermann, Helv. Phys. Acta **30**, 407 (1957).
- [6] S. Laporta and E. Remiddi, Phys. Lett. B **265**, 182 (1991); **356**, 390 (1995); **379**, 283 (1996); S. Laporta, Phys. Rev. D **47**, 4793 (1993); Phys. Lett. B **343**, 421 (1995).
- [7] J. A. Mignaco and E. Remiddi, Nuovo Cimento **60A**, 519 (1969);
- [8] T. Kinoshita, J. Math. Phys. **3**, 650 (1962).
- [9] J. Aldins, T. Kinoshita, S. J. Brodsky, and A. J. Dufner, Phys. Rev. Lett. **23**, 441 (1969); J. Aldins, T. Kinoshita, S. J. Brodsky, and A. J. Dufner, Phys. Rev. D **1**, 2378 (1970).
- [10] W. Czyz, G. C. Sheppey, and J. D. Walecka, Nuovo Cim. **34**, 404 (1964).
- [11] S. J. Brodsky, and T. Kinoshita, Phys. Rev. D **3**, 356 (1971).
- [12] P. Cvitanovic and T. Kinoshita, Phys. Rev. D **10**, 3991 (1974).
- [13] P. Cvitanovic and T. Kinoshita, Phys. Rev. D **10**, 4007 (1974).
- [14] SCHOONSCHIP was originally written by M. Veltman. Later improved by H. Strubbe, Compt. Phys. Commun. **8**, 1 (1974); **18**, 1 (1979).
- [15] J. A. M. Vermaseren, FORM ver. 2.3 (1998).
- [16] G. P. Lepage, J. Comput. Phys. **27**, 192 (1978).
- [17] T. Kinoshita and M. Nio, Phys. Rev. Lett. **90**, 021803 (2003).

- [18] T. Kinoshita, Phys. Rev. Lett. **75**, 4728 (1995).
- [19] S. Laporta, hep-ph/010233; Anastasiou and Lazopoulos, hep-ph/0404258; A. Smirnov and M. Steinhauser, Nucl.Phys. B **672**, 199 (2003).
- [20] M. Caffo, S. Turrini, and E. Remiddi, Phys. Rev. D **30**, 483 (1984); E. Remiddi and S. P. Sorella, Lett. Nuovo Cimento **44**, 231 (1985).
- [21] T. Kinoshita and W. B. Lindquist, Phys. Rev. D **27**, 867 (1983); **27**, 877 (1983); **27**, 886 (1983); **39**, 2407 (1989); **42**, 636 (1990).
- [22] T. Kinoshita, *Theory of the Anomalous Magnetic Moment of the Electron – Numerical Approach*, in *Quantum Electrodynamics*, editor T. Kinoshita (World Scientific, Singapore, 1990), pp. 218 - 321.
- [23] T. Kinoshita, IEEE Trans. Instrum. Meas. **44**, 498 (1995).
- [24] T. Kinoshita, IEEE Trans. Instrum. Meas. **46**, 108 (1997).
- [25] T. Kinoshita, IEEE Trans. Instrum. Meas. **50**, 568 (2001).
- [26] V. W. Hughes and T. Kinoshita, Rev. Mod. Phys. **71**, S133, (1999).
- [27] T. Kinoshita, *Anomalous Magnetic Moment of the Electron and the Fine Structure Constant in An Isolated Atomic Particle at Rest in Free Space: Tribute to Hans Dehmelt, Nobel Laureate*, editors: E. N. Fortson and E. M. Henley, (Narosa Publishing House, New Delhi, India, 2005).
- [28] T. Kinoshita, *Recent Developments of the Theory of Muon and Electron $g-2$* , in “*In Memory of Vernon Willard Hughes*”, editors: E. W. Hughes, F. Iachello (World Scientific, Singapore, 2004), pp. 58 - 77.
- [29] T. Kinoshita, Nucl. Phys. B (Proc. Suppl.) **144**, 206 (2005).
- [30] T. Kinoshita and M. Nio, Phys. Rev. D **70**, 113001 (2004).
- [31] P. J. Mohr and B. N. Taylor, Rev. Mod. Phys. **77**, 1 (2005).
- [32] T. Kinoshita and M. Nio, in preparation.
- [33] T. Aoyama, M. Hayakawa, T. Kinoshita, and M. Nio, in preparation.
- [34] M. A. Samuel and G. Li, Phys. Rev. D **44**, 3935 (1991); Phys. Rev. D **48**, 1879(E) (1991); G. Li, R. Mendell, and M. A. Samuel, Phys. Rev. D **47**, 1723 (1993); A. Czarnecki and M. Skrzypek, Phys. Lett. B **449**, 354 (1999); S. Laporta, Nuovo Cim. **A106**, 675 (1993); S. Laporta and E. Remiddi, Phys. Lett. B **301**, 440 (1993); B. Lautrup, Phys. Lett. **69B**, 109 (1977).
- [35] Private communications, F. Jegerlehner and B. Krause, 1996.
- [36] A. Czarnecki, B. Krause, and W. J. Marciano, Phys. Rev. Lett. **76**, 3267 (1996).

- [37] A. Wicht *et al.*, in *Frequency Standards and Metrology*, Proc. of 6th Symposium, University of St Andrews, Fife, Scotland, 9-14 September 2001. Ed. P. Gill (World Scientific, Singapore, 2002), pp. 193 - 212.
- [38] T. Udem *et al.*, Phys. Rev. Lett. **82**, 3568 (1999).
- [39] G. Källén and A. Sabry, Dan. Vidensk. Selsk. Mat.-Fys. Medd. **29**, No. 17 (1955).
- [40] A. H. Hoang *et al.*, Nucl. Phys. B **452**, 173 (1995).
- [41] D. J. Broadhurst, A. L. Kataev, and O. V. Tarasov, Phys. Lett. B **298**, 445 (1993); P. A. Baikov and D. J. Broadhurst, in Proceedings of the 4th International Workshop on Software Engineering and Artificial Intelligence for High Energy and Nuclear Physics (AIHENP95), Pisa, Italy, 1995, p.167 [arXiv:hep-ph/9504398]
- [42] T. Kinoshita and W. J. Marciano, *Theory of the Muon Anomalous Magnetic Moment in Quantum Electrodynamics*, edited by T. Kinoshita (World Scientific, Singapore, 1990), pp. 419 - 478.
- [43] M. Caffo, E. Remiddi, and S. Turrini, Nucl. Phys. B **141**, 302 (1978); J. A. Mignaco and E. Remiddi, 1969, unpublished.
- [44] Note that $P(P4, P2)$ is simplified to $P4(P2)$.
- [45] S. Laporta and E. Remiddi, Phys. Lett. B **301**, 440 (1993).
- [46] T. Kinoshita and W. B. Lindquist, Phys. Rev. D **39**, 2407 (1989).
- [47] We thank T. Aoyama for providing us with the translation code.
- [48] R. Sinkovits, unpublished.
- [49] L. D. Landau, Nucl. Phys. **13**, 181 (1959); J. D. Bjorken, Stanford University preprint (1959); N. Nakanishi, Progr. Theoret. Phys. **22**, 128 (1959).
- [50] Y. Hida, X. S. Li, and D. H. Bailey, Quad-double arithmetic: Algorithm, implementation, and application. Technical Report LBNL-46996, Lawrence Berkeley National Laboratory, Berkeley, CA 94720, October 2000. Available at <http://www.nersc.gov/~dhbailey/mpdist/mpdist.html>.